Paleoceanography and Paleoclimatology

AGU ADVANCING EARTH AND SPACE SCIENCES

RESEARCH ARTICLE
10.1029/2023PA004741

Special Section:
Illuminating a Warmer World: Insights from the Paleogene

Palynofloral Change Through the Paleocene-Eocene Thermal Maximum in the Bighorn Basin, Wyoming

Vera A. Korasidis[1,2] **and Scott L. Wing**[2]

[1]School of Geography, Earth and Atmospheric Sciences, The University of Melbourne, Parkville, VIC, Australia, [2]Department of Paleobiology, National Museum of Natural History, Smithsonian Institution, Washington, DC, USA

Key Points:

- Bighorn Basin palynofloras began shifting toward hot/dry tolerant plants during the latest Paleocene "pre-onset" carbon isotope excursions
- Palynofloras from early in the carbon isotope excursion (CIE)-body were dominated by ferns and palms indicating disturbance, then later by dry tropical lineages
- Wetland taxa regained abundance during the CIE recovery, indicating climate-forced changes in plant distributions without major extinction

Supporting Information:

Supporting Information may be found in the online version of this article.

Correspondence to:

V. A. Korasidis,
vera.korasidis@unimelb.edu.au

Citation:

Korasidis, V. A., & Wing, S. L. (2023). Palynofloral change through the Paleocene-Eocene Thermal Maximum in the Bighorn Basin, Wyoming. *Paleoceanography and Paleoclimatology*, *38*, e2023PA004741. https://doi.org/10.1029/2023PA004741

Received 14 AUG 2023
Accepted 14 NOV 2023

Abstract To better understand the effect of the Paleocene-Eocene Thermal Maximum (PETM) on continental ecosystems, we studied 40 new palynological samples from the Bighorn Basin (BHB), northwestern Wyoming, USA. We see palm and fern abundances increase in the last 20–40 ka of the Paleocene, then dramatically with the onset of the carbon isotope excursion (CIE) defining the base of the PETM. Palynomorphs of plant groups with modern temperate climate distributions are absent from the CIE body, and this is when tropical plants are most diverse and abundant. During the CIE recovery, pollen of mesophytic/wetland plants become more common while tropical taxa persist. In the post-CIE early Eocene tropical taxa are rare and temperate forms abundant, similar to the late but not latest Paleocene. Changes in the palynoflora are more easily detected if reworked palynomorphs are removed from analyses. We interpret palynofloral changes to indicate warming in the latest Paleocene, rapid warming and drying with the CIE onset, dry tropical climates through the CIE body, a return to wetter floodplains during a very warm CIE recovery, and cooler wet conditions in the post-PETM early Eocene. These inferences are consistent with geochemical and paleobotanical proxies. Strikingly similar patterns in the palynoflora and megaflora suggest changes in vegetation were a basin-wide phenomenon. These rapid, climatically forced changes in floral composition occurred without major extinction, perhaps indicating nearby refugia in which plants adapted to cooler and wetter climates persisted through the PETM.

1. Introduction

The Paleocene-Eocene Thermal Maximum, or PETM, was a period of elevated global temperature, ocean acidification and biotic turnover during the initial 150–200 ka of the Eocene (Gutjahr et al., 2017; Kennett & Stott, 1991; Zachos et al., 1993, 2003). The PETM was caused by the release of thousands of Pg of isotopically light carbon in a period of ∼5 ka, commonly known as the onset of the Carbon Isotope Excursion (CIE). The CIE onset was followed by an ∼100 ka-long period of approximately constant carbon isotope composition known as the CIE body, and a shorter interval of 40–80 ka during which carbon isotope values returned to background levels, known as the CIE recovery (Bowen et al., 2006; McInerney & Wing, 2011; Sluijs et al., 2007). Carbon release during the PETM caused global change not only in temperature (Cramwinckel et al., 2018; Dunkley Jones et al., 2010, 2013; Inglis et al., 2020; Tierney et al., 2022; Zhu et al., 2019), but also the distribution of precipitation (Carmichael et al., 2017, 2018), and terrestrial biomes (Korasidis, Wing, Shields, & Kiehl, 2022).

The most studied continental record of the PETM is preserved in the Fort Union and Willwood formations of the Bighorn Basin (BHB), northwestern Wyoming (e.g., Clyde & Gingerich, 1998; Fricke et al., 1998; Gingerich, 2003; Koch et al., 1992; Kraus & Riggins, 2007; Kraus et al., 2013; Magioncalda et al., 2004; Secord et al., 2010; F. A. Smith et al., 2007; Wing et al., 2005, 2009). Prior paleobotanical research on megafloras across the PETM in the BHB showed major and rapid change in floral community composition across the hyperthermal (Wing & Currano, 2013; Wing et al., 2005, 2009). Megafossil assemblages from the CIE body are dominated by Fabaceae, Arecaceae, and Hernandiaceae, taxa whose living members are important in tropical and subtropical areas, while assemblages from the late Paleocene and post-PETM early Eocene are dominated by Platanaceae, Hamamelidaceae, Betulaceae, Cercidiphyllaceae, Cupressaceae and other groups with many living members in temperate regions (F. A. Smith et al., 2007; Wing, 1998; Wing & Currano, 2013; Wing et al., 2005, 2009). Species belonging to these temperate-climate groups are notably absent from the CIE body.

Palynofloras from the same stratigraphic sections that produced the megafossil record, in contrast, showed relatively modest change across the PETM. Initially samples from the PETM itself were lacking, and though there

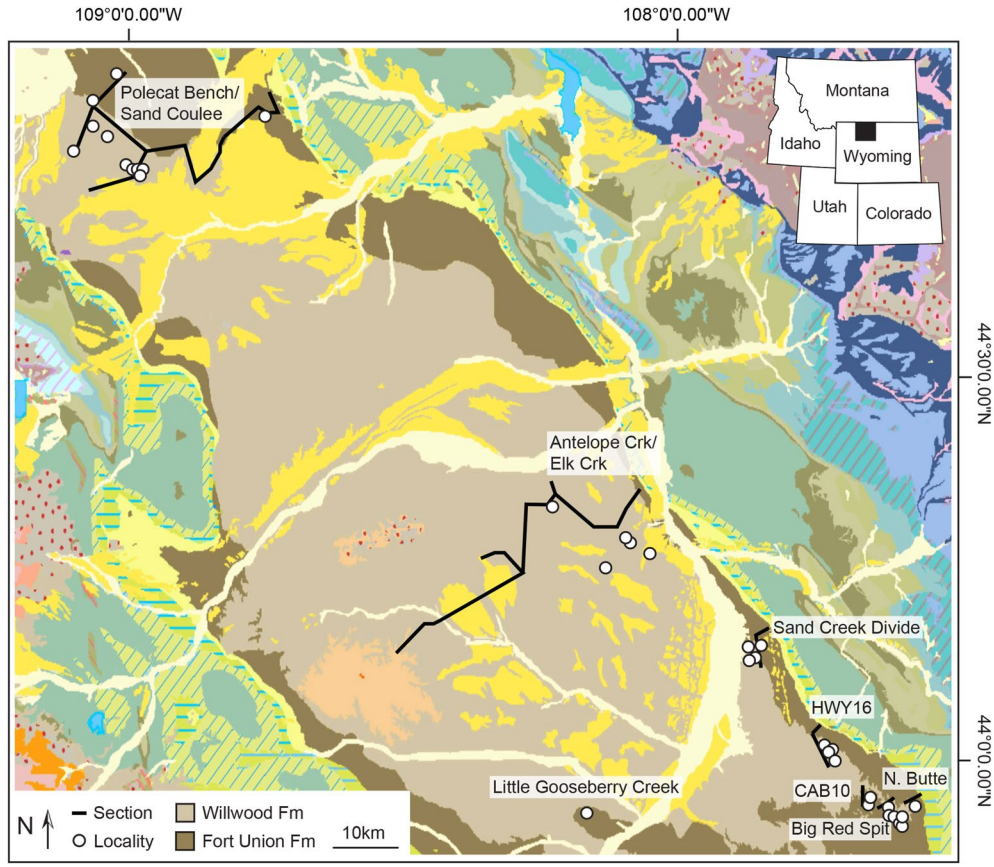

Figure 1. Map of field area in the Bighorn Basin. Circles designate locations of palynological samples in this study. Black lines indicate lines of composite sections shown in Figure 2. Base map from Love and Christiansen (1985). Fort Union Fm outcrop is brown, Willwood Fm is tan, Quaternary alluvium yellow, and green shades toward basin margins are various Cretaceous formations.

were notable immigrant taxa in the early Eocene (e.g., *Platycarya platycaryoides*, *Intratriporopollenites instructus*), palynofloras from before and after the event were similar at the family level, being dominated by Juglandaceae, Betulaceae, Fagaceae, Platanaceae, and Cupressaceae (Harrington, 2001; Wing & Harrington, 2001). Later, two pollen samples were recovered from the PETM of the BHB, and these contained rare grains of pollen types more commonly found in the Paleocene-Eocene of the Gulf Coastal plain (e.g., *Brosipollis*, Bombacoideae), but also a substantial number of grains belonging to long-ranging Paleocene and post-PETM Eocene taxa (Wing et al., 2005). Recently we showed that there was a major increase in reworked pollen during the CIE body, probably reflecting enhanced erosion and redeposition by fluvial systems responding to a highly variable precipitation regime (Korasidis, Wing, Nelson, & Baczynski, 2022). Here we re-examine palynofloral change across the PETM using 40 samples (including newly processed samples from the original two sites), many from the CIE body. We re-examine floristic change across the PETM as seen through the palynoflora and consider the climatic and ecological implications.

2. Materials and Methods

2.1. Geological and Sedimentological Setting

The NW-SE-oriented Bighorn Basin (BHB) contains thousands of square kilometers of exposures of the Paleocene Fort Union Formation and Paleocene-Eocene Willwood Formation, which were deposited by fluvial systems with headwaters in the adjacent uplifts of the Bighorn, Owl Creek and Beartooth Mountains (Figure 1; Bown, 1980). The palynofloral samples we describe here were collected from five types of fluvial subenvironments characterized by differences in grain size, primary bedding, cross-sectional geometry, and proximity to paleochannels

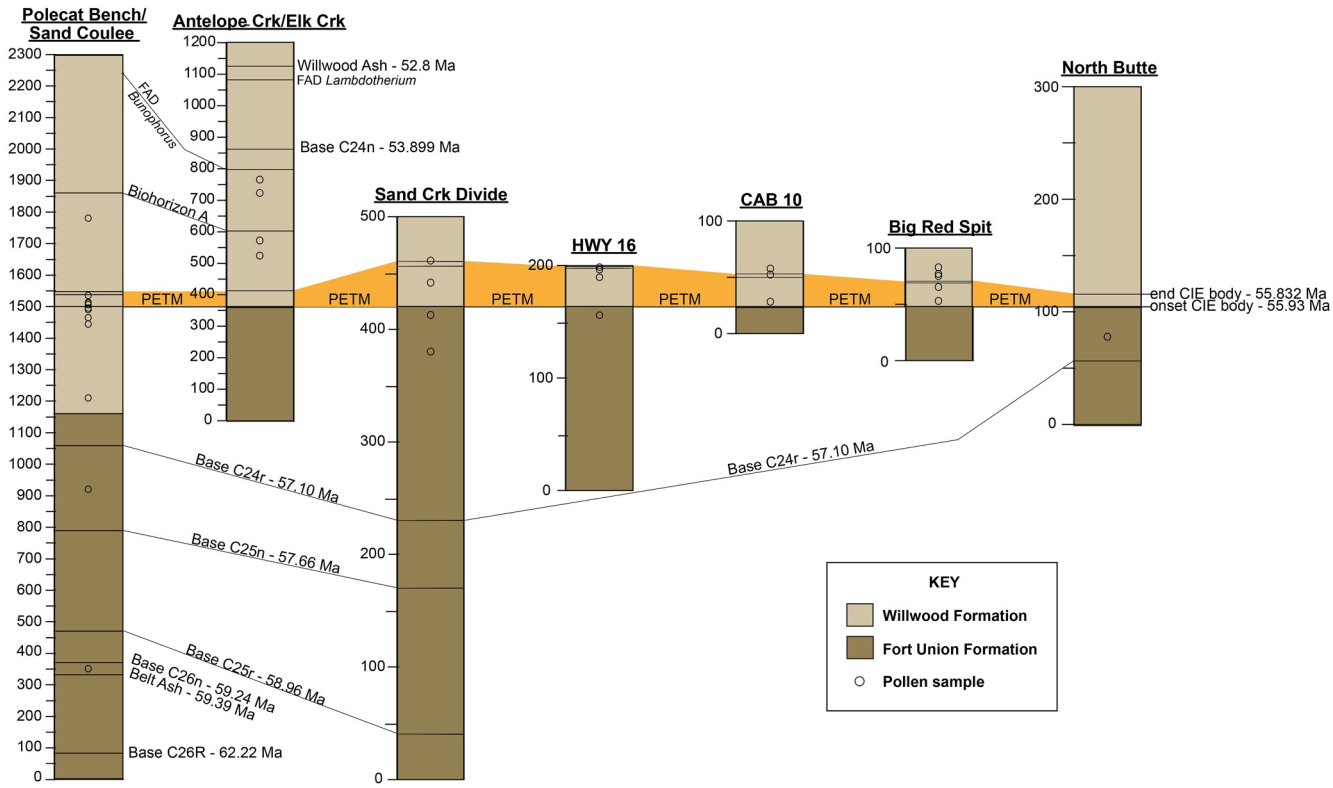

Figure 2. Composite stratigraphic sections through the Fort Union and Willwood Formations in the Bighorn Basin showing meter levels of pollen samples as well as biostratigraphic, paleomagnetic and radiometric levels used for correlation and age calibration. Sections are arranged from northwest (L) to southeast (R) and the reference level is the base of the carbon isotope excursion (CIE). Note, the Polecat Bench/Sand Coulee and Antelope Creek/Elk Creek sections are plotted at a smaller scale than the other sections. The Paleocene-Eocene Thermal Maximum (PETM), highlighted in orange, is recognized by the negative CIE and vertebrate fossils (biozone Wa-0). Closely spaced horizontal lines near the top of the PETM mark the end of the body (lower) and the end of the rapid recovery interval of the CIE (lower), but are not identified in all sections. The pollen sample from Little Gooseberry Creek is not shown because there is no measured section, although faunal and isotope stratigraphy clearly indicate it is from the PETM.

(Davies-Vollum, 2001; Davies-Vollum & Wing, 1998; Farley, 1989; Harrington, 2001; Korasidis, Wing, Nelson, & Baczynski, 2022; Wing, 1984): (a) laterally extensive backswamps, (b) abandoned channel fills, (c) crevasse splay channels, (d) in-channel mud drapes and scour fills, and (e) shallow floodplain lakes (Table S1). Palynofloras were preserved in all five subenvironments via rapid burial by one or more sedimentation events. The resulting palynofloral assemblages are likely dominated by local basinal and riparian vegetation but may include rare regional floral elements from surrounding uplifts arriving via water or wind (Farley, 1989, 1990; Jacobson & Bradshaw, 1981). Plant fossil bearing deposits of any type are relatively rare in the Willwood Formation because of widespread pedogenic oxidation of the floodplain deposits (e.g., Bown & Kraus, 1981; Neasham & Vondra, 1972), which is why plant fossil records (including palynological) must be drawn from across the BHB.

In many parts of the BHB, the PETM has been identified as a 30–45 m thick sequence of fluvial rocks and paleosols at or near the formational contact. The samples for this study come from PETM exposures in the northwest, southeast and southern BHB (Figures 1 and 2). Within each area deposits are correlated lithostratigraphically by bed tracing and local measurement of stratigraphic sections. What would later be called the PETM was first recognized biostratigraphically in the northwestern BHB Polecat Bench-Sand Coulee (PCB-SC) region (Gingerich, 1989). There are currently three local sections in this region where the CIE associated with the PETM has been documented in pedogenic $CaCO_3$ nodules, mammalian tooth enamel, total organic carbon (TOC), or all three, and these three sections can also be correlated with one another lithostratigraphically and biostratigraphically (Bowen et al., 2001, 2015; Foreman, 2014; Gingerich & Clyde, 2001; Koch et al., 1992; Magioncalda et al., 2004; van der Meulen et al., 2020). Fourteen of the 40 samples discussed in this paper are from the PCB-SC region, with one from the Saddle Mountain local section (Foreman, 2014) and the remaining 13 from the Head of Big Sand Coulee local section (van der Meulen et al., 2020; see Table S1 for palynofloral sample information). The southeastern

BHB also has areally extensive outcrops representing the Paleocene-Eocene boundary interval, including the PETM (Baczynski et al., 2013). As in the northern BHB, the presence of the CIE has been demonstrated in a variety of materials including pedogenic $CaCO_3$ nodules, TOC, leaf waxes (*n*-alkanes), and mammalian tooth enamel (Baczynski et al., 2013, 2016; Clyde et al., 2013; Rose et al., 2012; Secord et al., 2012; Wing et al., 2005). Twenty of the palynofloral samples described here come from five sections that cross the PETM in the southeastern BHB: Sand Creek Divide, Highway 16 (Hwy 16), Cabin Fork 10 (CAB10), Big Red Spit, and North Butte (Figures 1 and 2). Five of the early Eocene, post-PETM palynofloral samples discussed in this paper come from the Antelope Creek-Elk Creek section in the eastern BHB (Bown et al., 1994; Clyde et al., 2007; Schankler, 1980; Wing, 1980). Finally, one palynofloral sample from the PETM (PS2005) comes from recently recognized PETM outcrops on Little Gooseberry Creek (LGC) in the south central BHB. No stratigraphic section has been published for LGC, but negative carbon isotope values characteristic of the CIE are present in pedogenic $CaCO_3$ nodules immediately underlying the palynofloral sample, the leaf fossil assemblage from the same bed has taxa characteristic of the CIE body, and the perissodactyl *Sifrhippus sandrae*, an index of the Wa-0 fauna found only within the CIE body, occurs immediately above the palynofloral sample (Wing et al., 2021). With a stratigraphic section yet to be measured, but with indicators of the CIE body both above and below, we have approximated the temporal position of sample PS2005 from LGC as the midpoint of the CIE body.

The three phases of the CIE, onset, body and recovery, have been recognized in many BHB stratigraphic sections from multiple carbon-containing materials including TOC, leaf waxes (*n*-alkanes), mammalian tooth enamel and pedogenic carbonate nodules (Baczynski et al., 2013, 2019; Bowen et al., 2001, 2015; Foreman, 2014; Magioncalda et al., 2004; Rose et al., 2012; Secord et al., 2012). Durations of the CIE phases originally were estimated from orbitally-driven cycles of color change in carbonate sediments in deep marine cores (e.g., Li et al., 2022; Murphy et al., 2010; Röhl et al., 2007). Independent cyclostratigraphic analyses of paleosol color in fluvial sections in the PCB-SC region of the BHB have confirmed the same number of cycles observed in marine sections, strengthening the conclusion that the sedimentary cycles are generated by changes in insolation driven by periodic changes in the Earth's orbit (Aziz et al., 2008; van der Meulen et al., 2020; Westerhold et al., 2018).

2.2. Estimating the Ages of Palynological Samples

Because our palynofloral samples are drawn from three areas within the BHB that are separated from one another by areas lacking Paleocene-Eocene exposure, the most expedient way to bring the sites into a common framework is to convert the stratigraphic positions of samples to numerical ages. This is possible because each local area and section has two or more tie points to events of known geological age (Figure 2). We calculate the age of each sample by linear interpolation between two tie points assuming that rates of sediment accumulation were uniform over the long term. This assumption of uniform sedimentation rate breaks down at fine scales because, as in most fluvial systems, sediment was deposited in discrete flooding events that were followed by an interval of non-deposition and soil formation (e.g., Jerolmack & Sadler, 2007; Schumer & Jerolmack, 2009). The timescale at which the assumption of uniform sedimentation rate breaks down varies for reasons related to subsidence rate, fluvial depositional style, and other factors, but the "compensation time scale" (the time necessary for fluvial systems to level out depositional topography through channel avulsion and migration) is thought to place a lower limit on time resolution in fluvial systems (Foreman & Straub, 2017). Foreman and Straub (2017) estimated the compensation time scale of the BHB Paleocene-Eocene sequence to be $\sim 10^4$ years and suggested that paleoclimate fluctuations with a periodicity twice as long would likely be faithfully recorded. This is consistent with previous work attributing the cycles of soil redness in the BHB to the same precessional (~21ka) variability also seen in deep marine sections (Abels et al., 2013; Aziz et al., 2008; van der Meulen et al., 2020; Westerhold et al., 2018). Compensation time scales of 10 ka or less are also supported by the similar rates of sediment accumulation (0.3–0.7 m/ka) calculated across time durations ranging from >2 Ma to 20 ka (Abels et al., 2013; Clyde et al., 2007). The relative constancy of calculated sedimentation rates down to precessional time scales could mean even finer time resolution is possible, but here we do not interpret sub-precessional scale changes in the palynoflora, though stratigraphic superposition in local sections still gives the correct temporal sequence at this finer scale. Sections and tie points used in calculating the age of each sample are given in Figure 2 and Table S1.

2.3. Sample Processing

Palynofloras were recovered using palynological processing methods outlined in Korasidis et al. (2023). Specimens were observed at 1,000× magnification in transmitted light with a Nikon Eclipse 80i microscope

and through a 100× Plan Fluor objective (numerical aperture of 1.3) using Differential Interference Contrast where appropriate. For each sample, we identified and counted the first 200 palynomorphs encountered (for one sample $N = 400$ and for three samples $N = 100$; Table S2), and also visually assessed their preservation state to determine if they were autochthonous or reworked (criteria described in Korasidis, Wing, Nelson, & Baczynski, 2022). To increase the probability of finding rare species, an additional 50 transects were scanned for samples from the CIE body (see Table S3 for the palynotaxa identified in these scans). All residues and slides are housed in the Department of Paleobiology, National Museum of Natural History, Smithsonian Institution. For each sample we also measured grain size, weight percent TOC, $\delta^{13}C_{TOC}$, and for many samples $\delta^{13}C_{n\text{-}C29}$ (Table S1). Methods for these were previously reported in Korasidis, Wing, Nelson, and Baczynski (2022).

2.4. Statistical Analysis

All statistical analyses were performed in the program R version 1.2.5001 (R Core Team, 2022), and the scripts used to perform the analyses are in the supplemental materials for this article (Text S1 in Supporting Information S1). We visualized changes in palynofloral composition through time by generating pollen diagrams of common taxa (>5% in one or more samples) using the "rioja" package within R. This was paired with a hierarchical cluster analysis of Bray-Curtis distances among samples based on the common taxa and constrained by the stratigraphic order of samples. The clustering was performed with the "vegan" package. We also examined the similarity of samples in taxonomic composition using detrended correspondence analysis (DCA) in the "vegan" package. These analyses were completed on sample by taxon matrices using both presence/absence and relative abundance data.

We examined changes in palynofloral diversity at the scale of individual sites and also by pooling samples into four time bins: late Paleocene, CIE body, CIE recovery phase and post-PETM early Eocene. For individual samples we rarefied richness (number of taxa) and evenness (Shannon) using the number of palynomorphs counted as the indicator of sampling effort using the "iNEXT" package in R. We tested for significant differences in mean sample richness and evenness among time bins using ANOVA performed in the R base package. We compared diversity among the four time bins by rarefying the pooled samples, and also by bootstrapping species accumulation curves, generated in the "vegan" package, to highlight the effects of heterogeneity in sample composition within each time bin (β diversity).

We also examined the effect of the depositional environment on palynofloral composition using analysis of similarity (ANOSIM) as implemented in the "vegan" package to assess the statistical significance of a priori groups of sites. Our goal was to compare the relative power of bins based on sample age as opposed to bins based on depositional environment to predict sample groups determined from palynofloral composition. In the first ANOSIM, we assigned samples to four time bins: late Paleocene, CIE body, CIE recovery and early Eocene. In the second ANOSIM, we assigned samples to the five depositional environments: floodplain lakes, abandoned channels, crevasse splay channel, in-channel muds and backswamps. For both tests, we set ANOSIM to perform 999 iterations of a procedure in which sites were randomly assigned to groups, then Bray–Curtis distances within and between groups were compared between the randomly constituted and a priori groups. We also used canonical correspondence analysis (CCA) in the "vegan" package to explore the relationship of taxonomic composition to sample characteristics such as grain size, %TOC, and $\delta^{13}C$.

We also used ANOSIM to examine the importance of reworking for the taxonomic composition of samples (Table S2). We conducted ANOSIM as above using the four a priori time bin sample groups and the abundance matrix of samples by taxa with and without reworked grains (including Cretaceous taxa and those judged to be deteriorated using the criteria described by Korasidis, Wing, Nelson, & Baczynski, 2022). We hypothesized that removing the reworked grains would increase the significance of the relationship between the a priori time bins and groupings determined by floral similarity. We paired the ANOSIM analysis with nonmetric multidimensional scaling (NMDS) based on the same Bray-Curtis distances to visualize the groupings of sites in multivariate taxon space determined with and without reworked grains. We did so because ANOSIM, a non-parametric test, uses ranked dissimilarities to test if there a statistical difference between communities of two or more groups of samples. Because it uses ranked dissimilarities, it complements an NMDS plot, which is also rank-based and non-metric.

2.5. Nearest Living Relative (NLR) Analysis

To investigate the paleoclimatic implications of palynofloral change across the PETM we determined the living relatives (NLR) of each autochthonous spore and pollen taxon at the genus or higher level (Table S4), then performed a search in the *Global Biodiversity Information Facility* (GBIF) to find all records of the extant taxon. Procedures to filter the records and exclude cultivated specimens and other errors are described in more detail by Korasidis, Wing, Shields, and Kiehl (2022) but the methods are summarized briefly here.

For each extant genus or higher taxon we assigned each living species occurrence in GBIF to a Köppen-Geiger climate type (Köppen & Geiger, 1936) using the gridded data set provided by Beck et al. (2018). The 0.0083° resolution (approximately 1 km at the equator) of this global map is much higher than that available in earlier versions (Kottek et al., 2006), which improves classification accuracy particularly in regions with sharp spatial and/or elevation gradients in climate. The climate data used by Beck et al. (2018) were explicitly corrected for topographic effects. We used the Köppen-Geiger system in preference to climate variables such as mean annual or monthly mean precipitation and temperature because they well express the interaction of climatic variables that are important in influencing vegetation (Denk et al., 2013), and because we wished to avoid quantitative estimates of paleoclimatic variables (see below). The Köppen-Geiger system defines five major climate types: tropical (A), dry (B), temperate (C), continental (D) and polar (E). Thirty climate subtypes are defined using threshold values in the seasonality of temperature and precipitation in such a way that subtypes are usually dominated by one major vegetational type (Beck et al., 2018; Kottek et al., 2006). Critical values defining the boundaries of the climate types and subtypes are from Beck et al. (2018, Table 1).

For each genus or higher taxon we calculated the number of extant species occurring in each Köppen-Geiger climate subtype, removing climate subtypes present by virtue of a single occurrence because many of these were incorrectly located or were horticultural specimens. We then created a histogram for each higher taxon showing the number of its living species found in each Köppen-Geiger climate subtype—the species-level diversity of the taxon in climate space. These taxon-specific distributions in Köppen-Geiger climate space were then summed and relativized for all the NLRs to show the proportion of total NLR species diversity in each Köppen-Geiger subtype. The modal climate subtype is probably the best estimate of the paleoclimate, though we only illustrate the distribution of the 10 most common subtypes.

There are many sources of error in NLR-based estimates of paleoclimate, including misassignment of fossil taxa to extant groups, extant members of a lineage that have evolved different climate preferences from their fossil relatives, and extant NLRs with geographic distributions that do not reflect their climatic tolerances (e.g., Peppe et al., 2018; Wolfe, 1995). To reduce the chance of taxonomic misassignment, we have mostly used NLRs at the family or tribe rather than generic level. This avoids inferring overly specific climate types from fossil palynomorphs that resemble but do not belong within extant genera. Dispersed fossil pollen that has been assigned to extant genera frequently turns out to belong to an extinct lineage once it is found in situ and additional reproductive and vegetative characters are available for analysis (e.g., Manchester & Dilcher, 1997; Manchester et al., 2004; Zetter et al., 2011). Although using higher taxa as NLRs reduces the chance of assigning too narrow a climate envelope to the fossil, it of course reduces the precision of paleoclimate inferences because higher taxa have broader climatic distributions than individual genera within them.

We are not aware of any method for quantifying the major sources of error cited above that pertain to paleoclimatic estimates made with NLR methods. The error bars commonly presented for NLR-based paleoclimatic estimates rather reflect only the variability among NLRs in climatic distribution (e.g., Greenwood et al., 2005). Given our inability to properly quantify error in paleoclimate estimates we (regretfully) prefer to limit ourselves to the categorical representation of paleoclimate provided by the Köppen-Geiger system.

3. Results

We recovered palynofloras from 40 samples (12 late Paleocene, 13 from the CIE body, 9 from the CIE recovery, and 6 from the post-PETM early Eocene; Table S1) and counted a total of 7,900 grains, representing 106 taxa (6,526 autochthonous grains, 73 autochthonous taxa (Table S2)). An additional 650 slide transects, in which grains were not individually counted but only additional taxa recorded, were made on CIE body samples, revealing five additional taxa during the CIE body (Table S2).

10.1029/2023PA004741

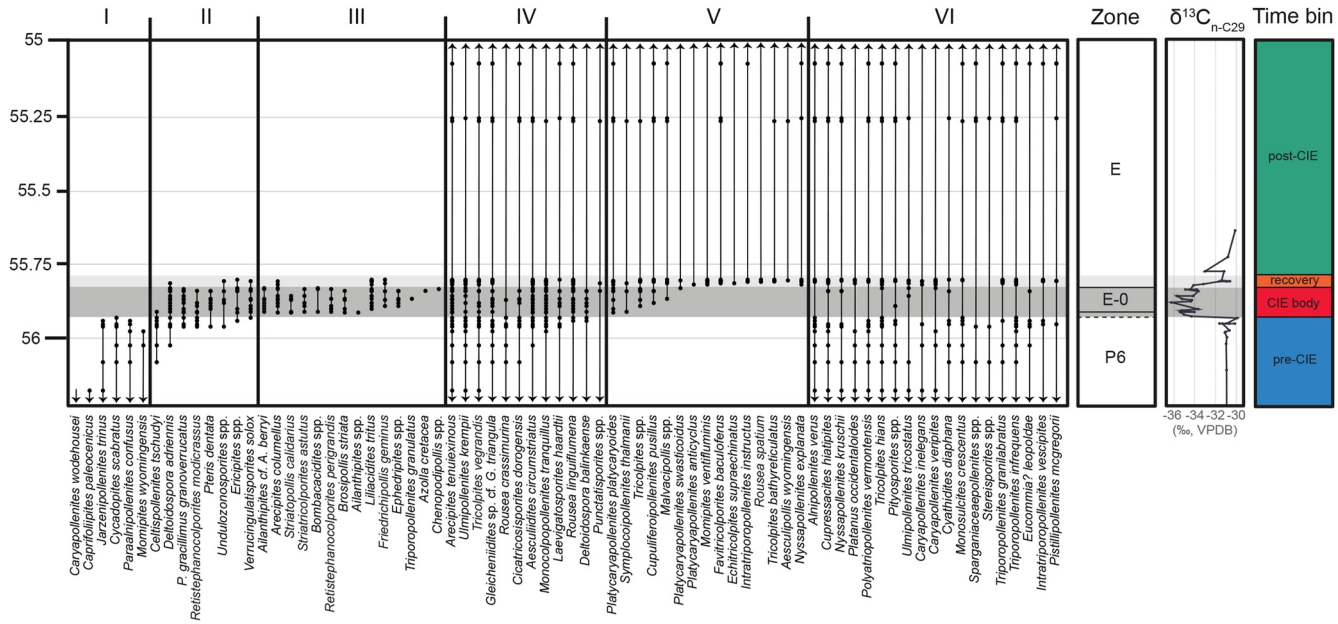

Figure 3. Temporal distributions of 73 species in the BHB during the Paleocene-Eocene transition. Species are grouped by temporal ranges as described in the text. Palynofloral zonation derived from Korasidis et al. (2023). $\delta^{13}C_{n\text{-}C29}$ of palynofloral samples derived from Korasidis, Wing, Nelson, and Baczynski (2022). The Carbon Isotope Excursion (CIE) is the negative shift in carbon isotope composition associated with the Paleocene-Eocene Thermal Maximum globally. The base of the CIE is placed at 55.93 (Westerhold et al., 2017) and the ages of samples were calculated by linear interpolation between tie points of known age using stratigraphic thickness (see Methods, Table S1).

3.1. Change in Palynofloral Composition Across the PETM

The temporal ranges of all 73 autochthonous taxa are plotted in Figure 3, arranged by first and last appearance datums (FAD and LAD). We recognize six groups of taxa that have different temporal distributions relative to the CIE. Group I taxa occur only in the Paleocene (6 taxa, 8% of flora), and four have last appearances in the final 100 ka of the Paleocene. Group II taxa (8, 11%) have first appearances late in the Paleocene (6 in the last 50 ka) and last appearances during the CIE body and/or CIE recovery. Group III taxa (14, 19%) occur only during the CIE body and/or CIE recovery. Group IV taxa (12, 16%) occur throughout the study sections before, during and after the CIE body. Group V taxa (15, 20%) first appear during the CIE body and/or CIE recovery and continue through the early Eocene. Group VI taxa (19, 26%) occur throughout the Paleocene and early Eocene, including the CIE recovery, but are very rare or absent during the CIE body. A total of 20 taxa have FADs in the CIE body, and an additional 9 have FADs in the CIE recovery. Thus, 40% of the autochthonous palynofloral assemblage first appears during the PETM.

The relative abundances of the 30 most abundant autochthonous taxa (>5% of the spore-pollen sum at ≥1 site; Figure 4), reveal some that have range gaps during the CIE body and others that have higher abundance during the CIE body. Those with high abundances during the CIE body include the palms *Arecipites tenuiexinous, Arecipites columellus* and *Monocolpopollenites tranquillus,* the pteridoid fern *Polypodiaceoisporites gracillimus granoverrucatus* and the eudicot *Aesculiidites circumstriatus* (Figure 4). Other common CIE body taxa include the ferns *Deltoidospora adriennis* and *Deltoidospora balinkaense* and the eudicots *Ailanthipites berryi* and *Rousea linguiflumena.* Paleocene assemblages instead are generally dominated by *Polyatriopollenites vermontensis* (Juglandaceae), but this taxon becomes increasingly rare in the Eocene. Samples from the CIE recovery also commonly contain abundant *Triporopollenites infrequens, Tricolpites hians* (Platanaceae) and *Triporopollenites granilabratus* whereas Eocene assemblages generally contain abundant *Alnipollenites verus* (Betulaceae), *Sparganiaceaepollenites sp. cf. Sparganium globites* and *Tricolpites vegrandis* (Platanaceae) pollen (Figure 4).

Gradients in palynofloral composition across the Paleocene-Eocene interval can be visualized through DCA of the abundance matrix which shows that the samples from the Paleocene, CIE body, CIE recovery and post-PETM Eocene occupy different regions of ordination space (Figure 5). The first and longest axis of the DCA separates samples from the CIE body from all others, reflecting both the taxa that have range gaps during the CIE body and those that are found exclusively during the CIE body (Figure 4). Although there is a large difference along Axis 1 between the youngest Paleocene sample (interpolated age 55.940 Ma) and the oldest sample within the

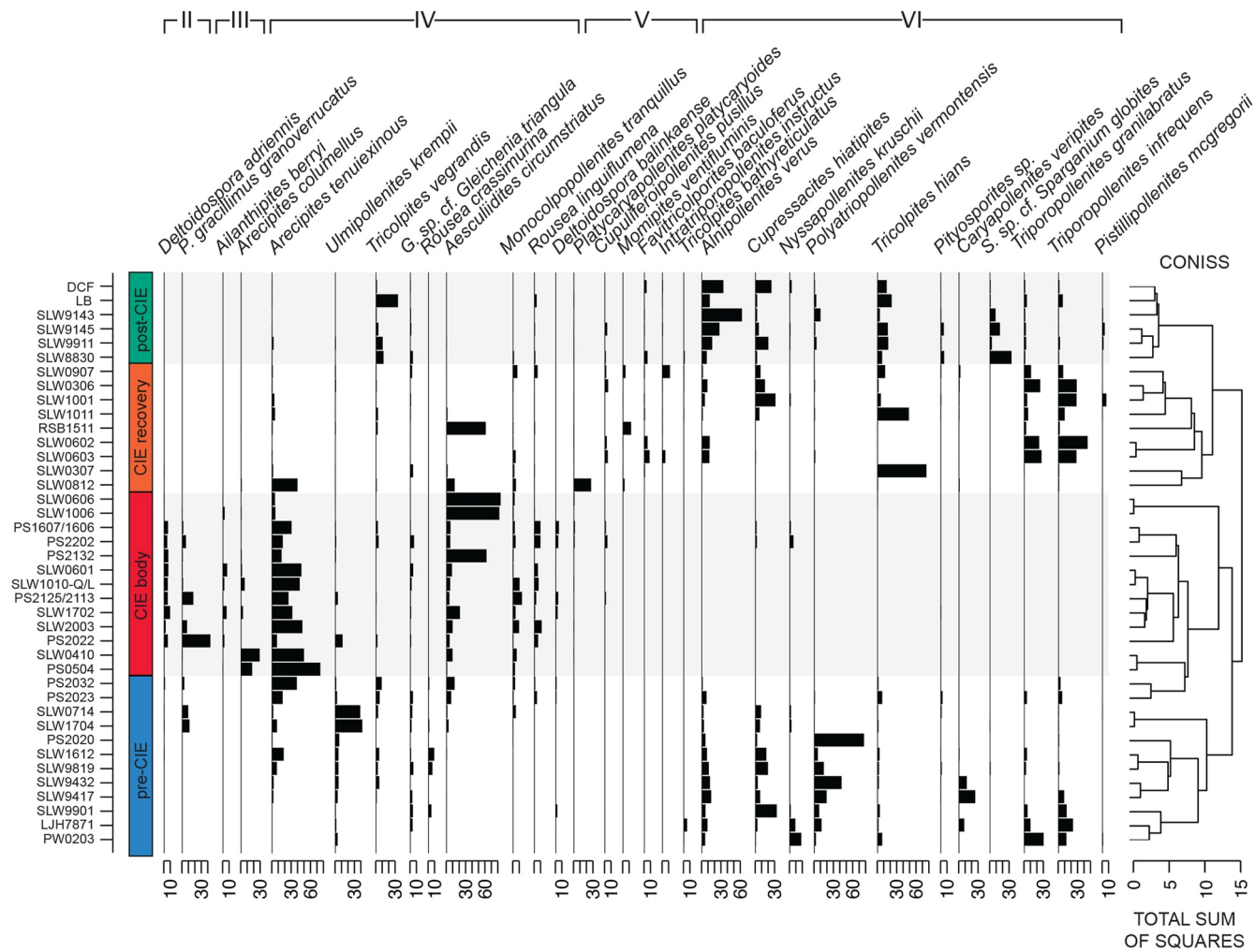

Figure 4. Pollen diagram and cluster analysis of BHB palynofloras. Pollen diagram based on the 30 palynotaxa that represent >5% of the spore-pollen sum at ≥1 site. Cluster analysis based on autochthonous grains only. Taxa are arranged along the *x*-axis in Groups II–VI as given in Figure 3.

body of the CIE (55.912 Ma), the four youngest Paleocene samples, all within 30 ka of the CIE onset, have Axis 1 scores intermediate between earlier Paleocene samples and those of the CIE body (Figure 5). The intermediate positions of these youngest four Paleocene samples reflects the first appearances of *D. adriennis* and *P. gracillimus granoverrucatus* (Figure 3) and the increased abundance of *A. tenuiexinous* and *A. circumstriatus* (Figure 4). Samples from the CIE body occupy a distinct region of the ordination, but interestingly the five CIE body samples from the southeastern part of the BHB are farthest right on Axis 1, and the five CIE body samples from the northwestern BHB are to the left, slightly closer to Paleocene and Eocene samples. The geographic subgrouping of samples from the CIE body in the ordination reflects the occurrence of certain fern spores (*Azolla cretacea, Cicatricosisporites dorogensis, Cyathidites diaphana, Deltoidospora adriennis, Punctatisporites* sp.), conifer pollen (*Cupressacites hiatipites, Pityosporites* sp.), and angiosperm pollen (*Cupuliferoipollenites pusillus, Eucommia leopoldae, Nyssapollenites kruschii, Symplocoipollenites thalmanii*) only in the northwestern BHB. Only southeastern BHB samples contain the angiosperms *Ailanthipites sp*., *Chenopodipollis sp*., *Rousea crassimurina*, *Triporopollenites granulatus*, and *Ulmipollenites tricostatus.* These differences in palynofloral composition are not related to the age of samples within the CIE body.

Samples from the CIE recovery occupy a broad spread along DCA Axis 1, overlapping with both CIE body samples and those of the Paleocene and post-PETM Eocene. Palms (*A. tenuiexinous*) and the eudicots *Aesculiidites circumstriatus*, *Platycarya platycaryoides*, and *Cupuliferoipollenites pusilus* are abundant in some CIE body and CIE recovery samples, but in general the CIE recovery samples are most like those

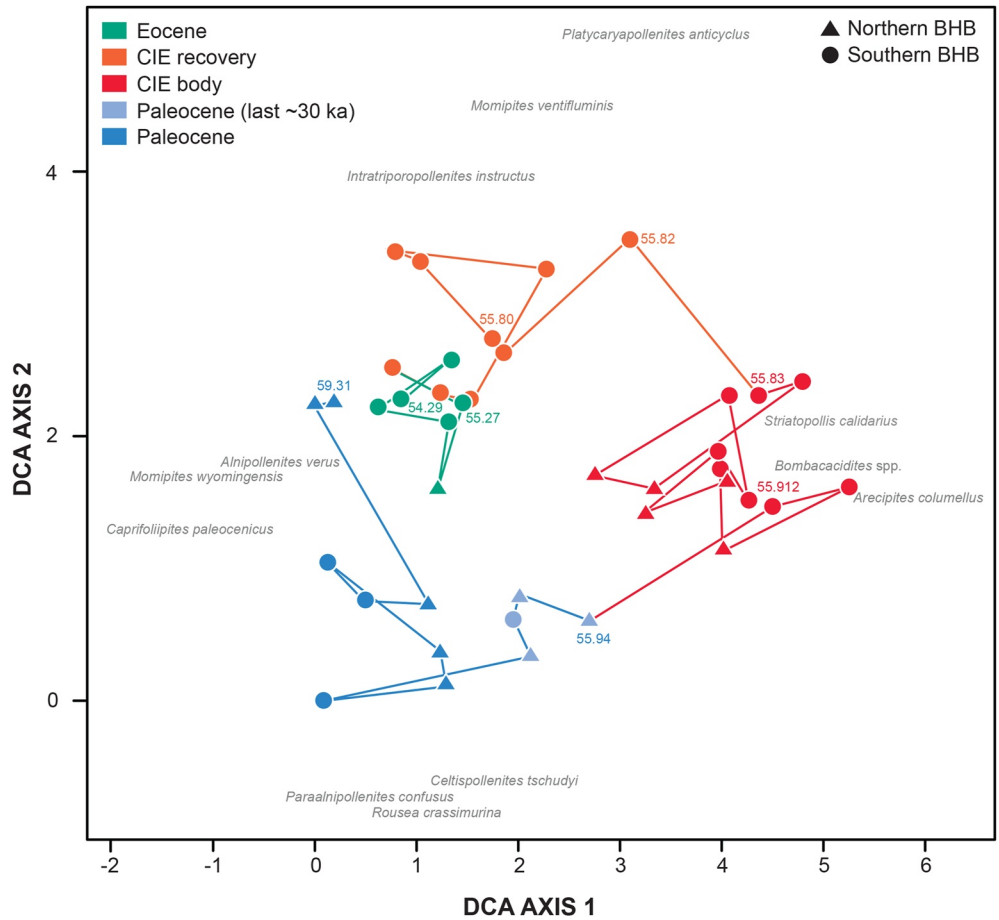

Figure 5. Change in palynofloral composition through the late Paleocene and early Eocene. Sample positions are from a detrended correspondence analysis (DCA) of the sites using the autochthonous species abundance matrix. Each symbol represents a palynofloral sample. Sites are coded by age bin, as indicated by color, and geographic subgrouping as indicated by symbol shape. The interpolated numerical ages of the first and last sample in each bin are given next to their symbols. Species positions are derived from the DCA biplot and each species label is centered at the coordinates for that taxon. Axis 1 corresponds largely to the compositional differences that distinguish Paleocene-Eocene Thermal Maximum samples from all others, whereas Axis 2 expresses differences between Paleocene and Eocene samples.

from the post-PETM early Eocene in the BHB in having abundant *Alnipollenites verus*, as well as common long-ranging forms such as *Triporopollenites infrequens, T. granilabratus, Tricolpites hians,* and *Cupressacites hiatipites* (Figures 4 and 5). The different palynofloral composition of Paleocene and post-PETM Eocene sites reflects both extinction/extirpation (Group I taxa) and numerous first appearances (Group V taxa) (Figures 3 and 4).

3.2. Change in Palynofloral Diversity Across the PETM

The mean rarefied richness of autochthonous taxa per sample (S_{50}) changes from 14.7 ± 1.1 in the Paleocene to 12 ± 1.4 during the CIE body, then to 11.2 ± 1.1 in the CIE recovery and 13.4 ± 1.0 in the post-PETM early Eocene (Table 1). ANOVA indicates there are not significant differences ($p = 0.169$) in rarefied sample richness among the time bins. The mean sample evenness expressed using Shannon Index is also highest in the Paleocene (9.2 ± 1.0), followed by the early Eocene (7.8 ± 1.0), CIE recovery (6.5 ± 1.2) and CIE body (6.5 ± 1.1) (Table 1). ANOVA indicates there are not significant differences in rarefied sample evenness among the time bins ($p = 0.211$). We also examined rarefied richness at larger sample standardization sizes, which reduced the total number of samples that could be used and found no significant differences in sample richness or evenness (Table 1).

Table 1
Mean and Standard Errors of Richness and Evenness of Paleocene-Eocene Palynofloras at the Scale of Samples and Time Bins

	Paleocene	CIE body	CIE recovery	Eocene
Number of samples	12	13	9	6
Number of grains	1,944	1,752	1,757	1,162
Mean observed sample richness, α	22	16	21	23.5
Mean rarefied sample richness, α_{50} ($N = 50$)	14.7 ± 1.1	12 ± 1.4	11.2 ± 1.1	13.4 ± 1.0
Mean rarefied sample richness, α_{150} ($N = 150$)	19.8 ± 1.8	18.2 ± 1.8	19 ± 1.9	21.3 ± 2.6
Mean rarefied sample Shannon Index ($N = 50$)	9.2 ± 1.0	6.5 ± 1.1	6.5 ± 1.2	7.8 ± 1.0
Rarefied time bin richness, γ_{1100} ($N = 1{,}100$)	45.2 ± 1.3	39.2 ± 1.2	43.6 ± 1.2	35.8 ± 1.9
Total observed time bin richness, γ	48	42	47	36
Beta diversity ($\beta = \gamma/\alpha$)	2.2	2.6	2.2	1.5

Note. We found no significant differences among time bins in mean sample richness or evenness, nor in the rarefied total richness or β-diversity of the four binned floras.

The richness of the pooled autochthonous flora of the late Paleocene time bin rarefied to 1,100 specimens is 45.2 ± 1.3 taxa. Rarefied richness of autochthonous palynomorphs decreases to 39.2 ± 1.2 in the CIE body, then increases to 43.6 ± 1.2 in the CIE recovery and decreases again to 35.8 ± 1.9 for the post-PETM early Eocene (Table 2; Figure 6a). A similar pattern emerges if richness is calculated by bootstrapping samples from each time bin rather than using analytical rarefaction of specimens in the pooled samples (Figure 6b). The species accumulation curves show the lowest richness and shallowest accumulation of species in the post-PETM early Eocene, with steeper curves for the Paleocene, CIE body and CIE recovery. The bootstrapped species accumulation curves for the time bins overlap broadly, suggesting no major differences in heterogeneity between the time bins. The similarity in beta diversity is also suggested by the β-diversity indices in Table 1. The additional 650 transects scanned for the CIE body sites (50 per site) resulted in species diversity increasing by five species after doubling the number of encountered autochthonous grains (a mean of 2.08 autochthonous grains were encountered per transect for the 13 CIE body sites, suggesting that an additional 1,352 autochthonous grains were encountered in the scans). This increase is at the upper end of the 95% confidence interval of the rarefaction curve—that is, new species were added at the upper end of the predicted rate based on the rate of encounter of new species in the full quantitative data set.

We also explored the fit of the count data summed by bin to various relative abundance distributions, and found that the Paleocene, CIE body and Eocene binned floras were all best fit by the Mandelbrot distribution, based

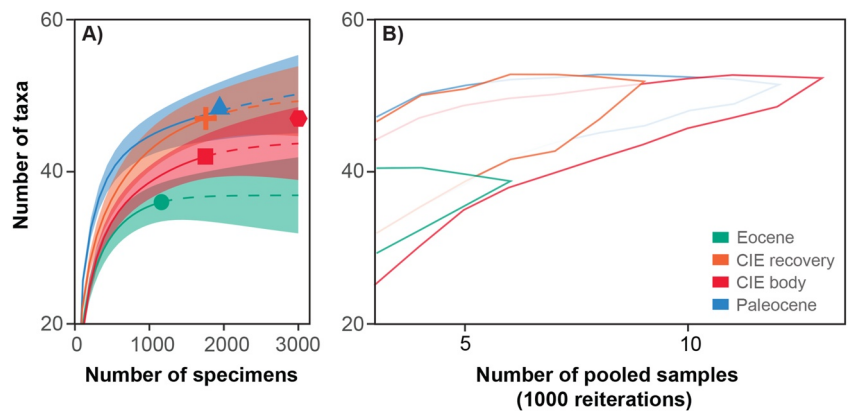

Figure 6. Comparison of diversity of Paleocene-Eocene time bins. (a) Rarefaction curves for pooled samples from each time bin. The solid lines are the mean values at the indicated sample size, the shaded areas are the 95% confidence intervals, and the dashed lines are extrapolations to the highest sample size for any time bin. The hexagonal symbol in red indicates the total number of taxa observed in all samples from the CIE body, which includes 650 slide transects in which grains were not individually counted but new taxa were noted, and for which we estimated the number of grains encountered from the density of palynomorphs on the slide. (b) Taxon accumulation curves for each time bin. The curves were calculated by randomly drawing the given number of samples and calculating total richness. Resampling was done with replacement and iterated 1,000 times for each number of samples. Enclosed areas give 95% confidence intervals. Steeper curves indicate greater heterogeneity among samples (β diversity).

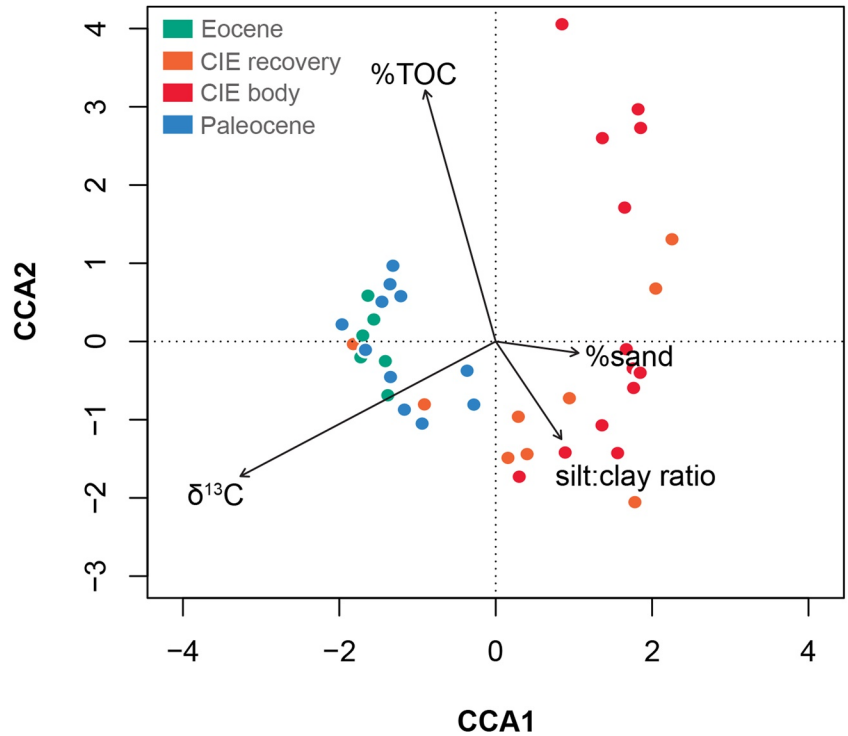

Figure 7. Canonical correspondence analysis (CCA) of BHB palynofloral samples. The CCA illustrates the relationship between gradients of palynofloral composition and four measured environmental variables: % total organic carbon (%TOC), $\delta^{13}C$, silt:clay ratio and % sand (see Table S1). Each symbol represents a sample, colored by time bin. The length of each environmental vector represents the strength of its relationship to palynofloral composition.

on the AIC score. The CIE recovery flora was slightly better fit by the preemption model distribution, with the Mandelbrot distribution a close second (Table S5).

3.3. Effect of Depositional Environments and Reworking on Palynofloral Composition

We conducted ANOSIM to determine the relative importance of depositional environments versus age in determining the taxonomic composition of samples across the data set. The four a priori sample groups based on age (Paleocene, CIE body, CIE recovery and post-PETM Eocene), had a strong and significant relationship with sample groupings based on taxonomic composition ($R = 0.57$, $P < 0.0001$). We also conducted ANOSIM on a priori groups of samples based on the five depositional environments (backswamps, abandoned channels, crevasse splays, in-channel muds, and floodplain lakes). Depositional groups were significantly but far less strongly correlated with taxonomic composition than were age-bin groups ($R = 0.10$, $P < 0.05$ for autochthonous specimens). In a third ANOSIM we used samples only from the abandoned channel environment and found that age bins were even more highly correlated with taxonomic composition, ($R = 0.78$ for autochthonous grains; $P < 0.0001$ for both analyses).

We assessed the relationship of palynofloral composition to measured features of the palynofloral samples through Canonical Correspondence Analysis (CCA; Figure 7). The features most strongly associated with palynofloral composition were $\delta^{13}C$ and %TOC. As expected, Paleocene and Eocene samples are associated with higher $\delta^{13}C$ and samples from the CIE body and CIE recovery with lower $\delta^{13}C$. Samples from the CIE body and CIE recovery tended to be associated with coarser grain size (%sand and silt:clay ratio) and lower %TOC, although a subset of seven samples from the CIE body and CIE recovery were associated with relatively high %TOC.

We conducted ANOSIM to test the relative importance of reworking in determining the taxonomic composition of samples across the abundance data set. The relationship between age-based groups and floral composition was slightly stronger when reworked specimens were excluded from the matrix used in ANOSIM ($R = 0.61$, $P < 0.0001$ vs. $R = 0.57$, $P < 0.0001$). When reworked specimens were excluded, the a priori groups based

Table 2
Analysis of Similarity (ANOSIM) of Paleocene-Eocene Palynofloras, With and Without Reworked Palynotaxa, Showing That Age-Based Groups Are More Significantly Associated With Floral Composition Than Are Groups Based on Depositional Environment, and That the Autochthonous Palynoflora Is Slightly More Associated With Both Grouping Factors Than Is the Total Palynoflora Including Reworked Grains

	Autochthonous palynotaxa	*P*	All palynotaxa	*P*
ANOSIM (age-based groups)	0.61	<0.0001	0.57	<0.0001
ANOSIM (depositional environment groups)	0.10	<0.05	0.13	<0.02

on depositional environment were slightly more strongly correlated with taxonomic composition than when reworked specimens were included ($R = 0.10$, $P < 0.05$ for only autochthonous grains; $R = 0.13$, $P < 0.02$ with reworked specimens included; Table 2). We also used NMDS on abundance matrices to visualize the effect of reworked grains on the distinctness of sample groups based on age (Figure 8).

3.4. Changes in the Climatic Preferences of NLRs

The NLRs of the autochthonous palynofloral taxa are given in Table S4 and the key pollen types are illustrated in Korasidis et al. (2023). In the BHB, the Paleocene is characterized by high proportions of palynotaxa with living relatives in temperate oceanic/subtropical montane climates (Cfb) and humid continental climates (Dfb) (Figure 9). These climate types are characterized by precipitation that is equally distributed across the year. During the CIE body there is an increase in palynotaxa with living relatives diverse in tropical rainforest (Af), tropical monsoonal forest (Am), and/or tropical savanna (Aw) climate types, though the highest proportion of NLR diversity is still the Cfb climates. Precipitation occurs all year long in tropical rainforest climates (Af), whereas in tropical monsoonal forest (Am) one or more months receive less than 60 mm of precipitation, and in tropical savanna (Aw) there are at least 2 months with less than 60 mm of precipitation. The proportion of NLRs occupying colder climate types decreases during the CIE body. During the CIE recovery the proportion of NLRs with tropical distributions declines from the higher levels of the CIE body; the Cfb climate zone retains the highest proportion of NLR diversity of any climate type. The proportion of NLR species in colder climates increases from that in the CIE body, but not to Paleocene levels. Like the other time bins, post-PETM early Eocene palynofloras have the highest proportion of NLR diversity in Cfb climates, but the proportion of NLR diversity in tropical zones decreases to the lowest level in the BHB record, and NLRs from cold climate zones have the highest proportion for any of the time bins (Figure 9).

4. Discussion

The results presented here demonstrate large and rapid changes in floral composition across the PETM in the Bighorn Basin, especially during the quasi-stable interval of unusually negative carbon isotope

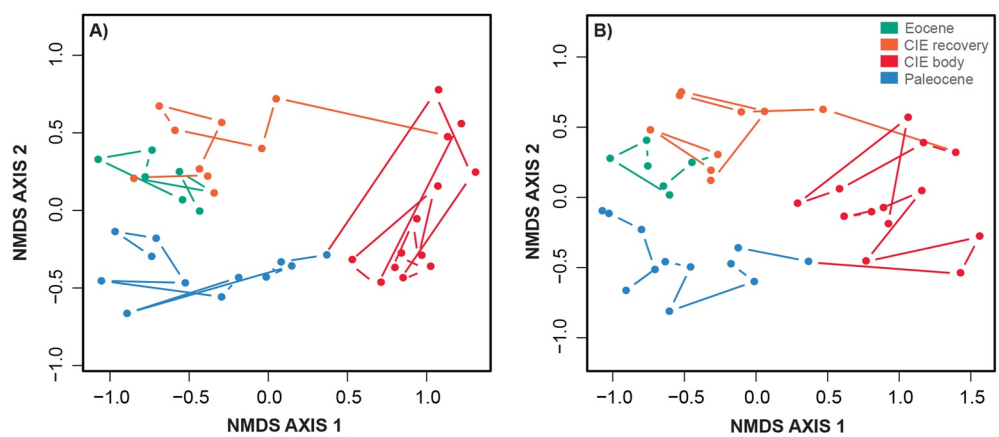

Figure 8. NMDS ordinations of the sample by species abundance matrix using: (a) all specimens. (b) only grains judged autochthonous by the criteria of Korasidis, Wing, Nelson, and Baczynski (2022). Sites are coded by age-bin as indicated in the key; lines connect samples in sequence by age. When reworked grains are excluded (b), samples from each age bin occupy slightly more distinct regions of the ordination.

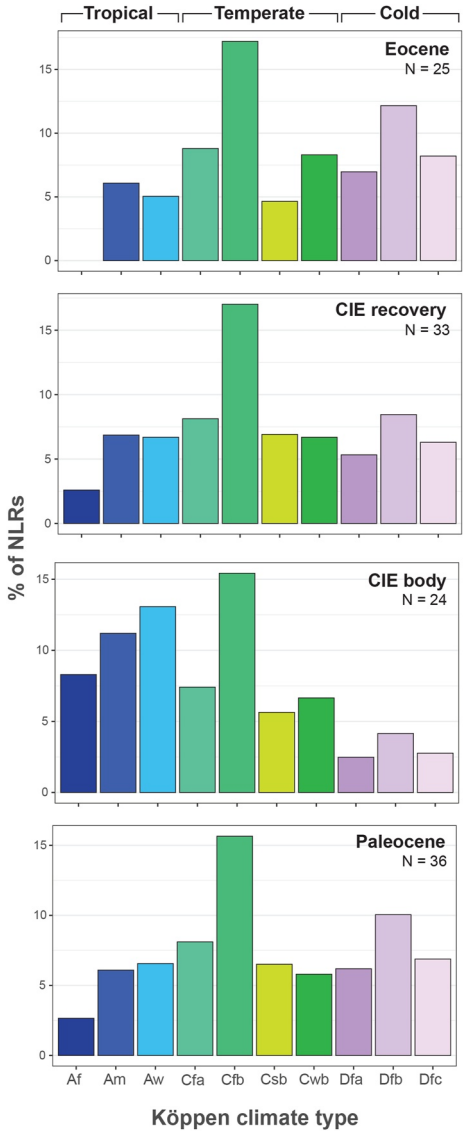

Figure 9. Köppen-Geiger climate type distributions of the Bighorn Basin palynofloras from the Paleocene, carbon isotope excursion (CIE) body, CIE recovery and post-PETM Eocene. The *y*-axis is the percent of the Nearest Living Relative species diversity of all fossil taxa in each of 10 Köppen-Geiger climate types. *N* is the number of fossil taxa. Af—tropical rainforest, Am—tropical monsoonal forest, Aw—tropical savanna, Cfa—temperate with no dry season and hot summer, Cfb—temperate with no dry season and warm summer, Csb—temperate with dry, warm summer, Cwb—temperate with dry winter, warm summer, Dfa—continental with no dry season and hot summer, Dfb—continental with no dry season and warm summer, Dfc—continental with no dry season and cold summer.

values referred to as the CIE body. Although the general pattern and timing of floral turnover is consistent with previous work on megafloras and palynofloras (Harrington, 2001; Wing & Currano, 2013; Wing & Harrington, 2001; Wing et al., 2005), 30 new samples in the ~400 ka period including the PETM allow us to refine our understanding of the rate and paleoclimatic implications of this floral change, as well as to quantify the influences of reworking, depositional environment and within-basin heterogeneity.

4.1. Effect of Depositional Environments and Reworking on Palynofloras

Before discussing the floristic and climatic implications of the palynofloral record we consider the influence of reworked palynomorphs and shifts in depositional environments on the apparent magnitude and rate of change. Early work on palynofloral response to the PETM in the BHB noted the unexpected persistence of pollen of the largely temperate families Cupressaceae and Juglandaceae during the CIE body, when megafossils of these families were absent (Wing et al., 2005). One possible explanation for the discordance of micro- and megafloras was that Paleocene palynomorphs were being eroded and redeposited, thus creating false records of temperate families during the CIE body. This explanation was borne out when we found that the stable carbon isotopic composition of Cupressaceae and Juglandaceae pollen grains from the CIE body was the same as that of Paleocene grains of the same taxa, whereas the stable isotopic composition of palm pollen showed the −4‰ shift expected from the change in the isotopic composition of the atmosphere (Korasidis, Wing, Nelson, & Baczynski, 2022). Pollen judged reworked from carbon isotopic composition also had visual signs of degradation (Korasidis, Wing, Nelson, & Baczynski, 2022). This demonstrated that even in the BHB, with its high rates of sedimentation (~0.2–0.7 m/ka) and absence of long hiatuses (Aziz et al., 2008; Bowen et al., 2015; van der Meulen et al., 2020; Westerhold et al., 2018), reworking of palynomorphs created the false appearance that taxa preferring wet, warm-temperate climates persisted through the CIE body. Taxa such as Cupressaceae and Juglandaceae that were abundant in the late Paleocene are the ones most likely to be reworked, and they are more likely to confuse interpretations of presence/absence data, since reworked grains are not usually abundant. The ANOSIM and NMDS analyses presented in this paper, performed on relative abundance data both with and without reworked pollen, demonstrate that in general reworked grains only slightly reduce the distinctness of palynofloras from the CIE body (Table 2; Figure 8). This is both because reworked Paleocene grains are not highly abundant and because reworked Cretaceous palynomorphs are more often found in the CIE body than in other samples; the Cretaceous grains give palynofloras from the CIE body a distinct composition even though they do not reflect contemporaneous floral change.

Changes in fluvial systems and floodplain depositional environments associated with the PETM in the BHB (e.g., Foreman, 2014; Kraus & Riggins, 2007; Kraus et al., 2015; Ramos et al., 2022; Wing et al., 2009) could have altered palynofloral composition by changing the taphonomic processes that intrude between the production of pollen by plants and pollen recovery by acid maceration. We cannot assess the full set of taphonomic processes (e.g., pollen production, dispersal, transport and preservation), but the CCA analysis above (Figure 7) shows that floral composition is less correlated with sediment grain size (related to current energy) and total organic content (related to pollen preservation), than it is with $\delta^{13}C_{n\text{-alkane}}$ (related to whether the sample comes from the CIE). This suggests that depositional and preservational processes are less important than PETM climatic change in determining the composition of palynofloras

through time. This is also consistent with the DCA analysis, which shows samples group by time bin. ANOSIM also shows that time bins are far more correlated with palynofloral composition than are depositional environments, and that when only samples from the pond fill environment are considered, time bins are still highly correlated with floral composition. All of these analyses are consistent with the idea that turnover in palynofloral composition during the PETM reflects real and sudden floral change across the BHB rather than reworking or changing taphonomic modes and depositional environments alone.

4.2. Floristic and Climatic Change

Our results here provide the most temporally resolved record of continental floral change across the PETM yet achieved (Figure 10). The most striking feature of the palynofloral record is the highly distinctive composition of samples from the CIE body, which results both from absences of long-ranging Paleocene-Eocene taxa and appearances of short-ranging forms not otherwise found in the northern Rocky Mountains in the late Paleocene-early Eocene interval. This pattern of brief appearances and temporal range discontinuities (*sensu* Schankler, 1981) is also what makes the megaflora of the CIE body highly distinct (Wing & Currano, 2013). Temporal range discontinuities are seen in both autochthonous pollen and megafossils of Juglandaceae, Betulaceae, Platanaceae, and Cupressaceae, which are common in the latest Paleocene, absent from the CIE body, and present again beginning in the CIE recovery period. Finding the same pattern in the palynoflora and megaflora strongly suggests that populations of these families were extirpated throughout the BHB during the CIE body.

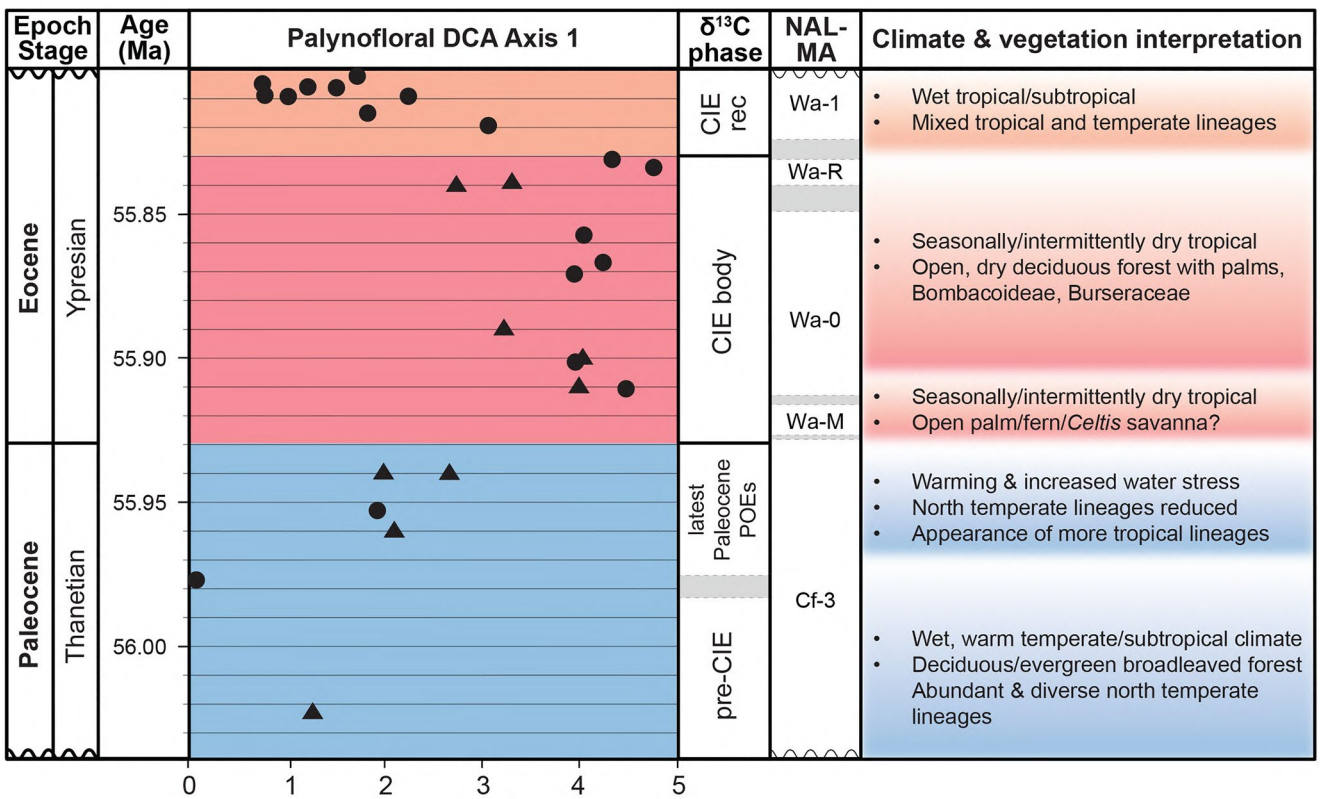

Figure 10. Changes in floral composition and inferred climate and vegetation for the Paleocene-Eocene Thermal Maximum (PETM) and latest Paleocene of the BHB. The *x*-axis on the left side is the first axis of the detrended correspondence analysis in Figure 5, which expresses the distinct floral composition of PETM floras. Black circles represent SE BHB samples. Black triangles represent NW BHB samples. North American Land Mammal Ages derived from van der Meulen et al. (2020). POE, pre-onset excursion. The ages of samples were calculated by linear interpolation between tie points of known age using stratigraphic thickness (see Methods, Figure 2, Table S1).

Late Paleocene (Thanetian, ~59–56 Ma) palynofloras from the BHB support previous paleobotanical and oxygen isotope work showing warm and humid climates in the BHB, with mean annual temperatures >15°C and mean annual precipitation >125 cm (Currano et al., 2008; Fricke & Wing, 2004; Wilf, 2000; Wing et al., 2005; Wing & Greenwood, 1993). *Polyatriopollenites vermontensis* was a persistent dominant (Figure 4) and is related to *Pterocarya* (family Juglandaceae, walnuts) (Pocknall & Nichols, 1996), a genus currently restricted to moist temperate to subtropical forests in Eastern Asia and Western Eurasia (Kozlowski et al., 2018; Zhang, Ree, et al., 2022). *Ulmipollenites krempii* was also abundant and is similar to extant *Planera* (Elsik, 1968), an extant genus in the temperate clade of Ulmaceae (elms) (Fragnière et al., 2021; Zhang, Deng, et al., 2022). *Cupressacites hiatipites* (Cupressaceae, bald cypresses) was likely derived from the genera *Metasequoia* (dawn redwood) and/or *Glyptostrobus* (swamp cypress) based on the ubiquitous co-occurrence of pollen and megafossils (Frederiksen, 1980; Pocknall, 1987); both genera grow in mesic to flooded habitats (Averyanov et al., 2009). Other important elements of the Thanetian palynoflora include *Alnipollenites verus* (*Alnus* in family Betulaceae, alders and birches; Nichols, 2010) and *Triporopollenites infrequens* (Betulaceae; Nichols & Brown, 1992), both of which commonly occupy inundated habitats in temperate regions (Furlow, 1979; Yang et al., 2022). Two members of the sycamore family Platanaceae are also found in most Thanetian samples: *Tricolpites hians* (possibly *Platanus*; Zavada & Dilcher, 1986; Denk & Tekleva, 2006), and *T. vegrandis* (associated with megafossils of *Macginitiea* and *Platananthus*; Manchester, 1986; Korasidis et al., 2023). Platanaceae today grow in warm to cool, wet climates (Feng et al., 2005; Nixon & Poole, 2003), and Paleocene megafossils are most common in proximal fluvial deposits (Wing, 1984). The highest diversity of living relatives of Thanetian plants from the BHB occur in Cfb (temperate oceanic) and Dfb (warm-summer, humid continental) Köppen climate types, supporting the wet, warm temperate to subtropical climatic interpretation (Figure 9).

Four samples from the latest Paleocene (last ~30 ka prior to the onset of the CIE) show the abundances of Juglandaceae, Betulaceae, Platanaceae, and Cupressaceae had already declined compared with older Thanetian samples, suggesting that reductions in their BHB populations may have preceded the onset of the CIE. These samples also record increased abundance of *Arecipites tenuiexinous*, (Arecaceae, palms; Nichols & Brown, 1992), *Polypodiaceoisporites gracillimus granoverrucatus* (similar to *Pityrogramma* in Pteridaceae, whose living species are in the American and Africa-Madagascan tropics; A. F. Tryon & Lugardon, 2012; R. M. Tryon & Tryon, 2012; Korasidis et al., 2023), and *Retistephanocolporites modicrassus* (similar to the extant genus *Ceiba*, tribe Bombacoideae, family Malvaceae, a large tree of the seasonally dry to wet tropics; Korasidis et al., 2023; Pezzini et al., 2021) (Figure 4). This latest Paleocene palynofloral change provides independent evidence for warming of ~5°C indicated by local isotopic and paleosol records (Kraus et al., 2013; Secord et al., 2010; Wing et al., 2009), and coincides with a series of short-lived negative excursions in the carbon isotope composition of pedogenic carbonate nodules, including the pre-onset excursion, or POE (Bowen et al., 2015; van der Meulen et al., 2020). Given the climatic preferences of their extant relatives, the increases in *R. modicrassus* and *P. g. granoverrucatus* may also indicate seasonal water stress and more open vegetation. These latest Paleocene samples show climate was changing prior to the onset of the CIE.

Although the latest Paleocene palynofloras are somewhat intermediate in composition between the earlier Thanetian and the PETM, the largest and most sudden change in floral composition through the ~5 million years discussed here occurs in between the last Paleocene and first PETM samples (Figure 10), which are, respectively, below and above the sudden onset of the CIE (Baczynski et al., 2013; Bowen et al., 2015; van der Meulen et al., 2020). This shift in floral composition, which occurred in ~30 ka or less, was the result of extirpations of long-ranging palynotaxa and most of the first appearances of the short-ranging PETM forms. The possibility of an even more rapid floral shift is left open because we lack palynofloras from the very lowest part of the CIE. In the NW BHB the lowest part of the CIE corresponds lithologically to the "Brown Beds," several distinctive, poorly-developed, sandy, brownish paleosols (Gingerich, 2001; Kraus & Riggins, 2007) that have not produced fossil pollen, although they produce abundant fossil endocarps of hackberry (*Celtis phenacodorum* Gingerich, 1989) and a distinctive mammalian fauna assigned to the *Meniscotherium* Zone (Wa-M of Gingerich, 2001; Gingerich & Smith, 2006). In the SE BHB the position of the Wa-M biozone is less clear because only a single *Meniscotherium* fossil is known and its exact stratigraphic position was not recorded at the time of collection (Strait, 2001). Our examination of exposures where it was found suggests it came from within or just below the Onset Geosol of Baczynski et al. (2013), which records the CIE onset in the SE BHB. The lowest palynofloral sample from the CIE in the SE BHB (PS0504) occurs in the mud fill of an ~1 m deep channel cut into the Onset Geosol, so is likely slightly younger than the Wa-M biozone. This is consistent with the occurrence in the upper part of the Onset Geosol of the lowest *Sifrhippus* (Perissodactyla), the index taxon of the succeeding Wa-0 faunal zone (Secord et al., 2012).

The plant extirpations at the onset of the CIE in the BHB were most likely caused by increased water stress. Both floral composition and physiognomy (this paper; Wing & Currano, 2013; Wing et al., 2005) indicate drier climates, and paleosol geochemistry, organic carbon content and paleosol morphology independently indicate better drained floodplain soils in the lower CIE than the latest Paleocene (Baczynski et al., 2016; Kraus & Riggins, 2007; Kraus et al., 2013; Woody et al., 2014). Regionally there is sedimentological evidence for higher variation and greater energy in streamflow during the CIE (Dechesne et al., 2020; Foreman, 2014; Foreman et al., 2012). All of these lines of evidence are consistent with intermittent, heavy precipitation events that are also predicted by climate modeling (Shields et al., 2021). There is also abundant isotopic evidence for increased temperature just before and during the CIE, both regionally (Fricke et al., 1998; Secord et al., 2010; Snell et al., 2013) and, of course, globally (e.g., Cramwinckel et al., 2018; Inglis et al., 2020; Jones et al., 2013; Tierney et al., 2022; Zhu et al., 2019). What BHB plants experienced as water stress may have been caused by less precipitation, more intermittent precipitation, higher evapotranspirative demand because of higher temperatures and lower humidity, or a combination of these factors. The large increase in atmospheric concentration of CO_2 during the CIE (e.g., Gutjahr et al., 2017; Haynes & Hönisch, 2020) would generally have been expected to increase water use efficiency because plants would be able to maintain carbon gain while reducing water loss through stomatal closure (e.g., Drake et al., 1997), thus decreasing transpiration rates and potentially increasing runoff (Betts et al., 2007). In spite of these expectations, the consistent magnitude of the CIE in BHB leaf waxes (e.g., Baczynski et al., 2016; F. A. Smith et al., 2007), pollen (Korasidis, Wing, Nelson, & Baczynski, 2022), tooth enamel (Koch et al., 1992; Secord et al., 2010) and also in planktic foraminifera (e.g., Kozdon et al., 2013) does not suggest a major decrease in photosynthetic discrimination against ^{13}C for BHB plants during the CIE, which would be expected if stomatal closure reduced transpiration and if water use efficiency increased. We note that recent work shows considerable diversity in stomatal response, including trees with limited water access that continue to transpire freely under elevated temperature and vapor pressure deficit (Marchin et al., 2023). Although we strongly favor water stress as the primary proximate cause of plant extirpations in the BHB during the CIE body, we do not have a means to disentangle the relative importance of the ultimate climatic stressors. Water stress was caused by some combination of increasing temperature, and decreasing water availability, which could have been intermittent, seasonal or year-round.

In light of the inferred importance of water stress in causing extirpations of plants in the BHB it is significant that in the Hanna Basin, ~250 km to the SE, landscapes remained wetter during the PETM (Azevedo-Schmidt et al., 2022), and some of the taxa that were locally extirpated during the CIE body in the BHB persisted through the same time in the Hanna Basin (Dechesne et al., 2020). Hanna Basin drainages may have been larger than those of the BHB, maintaining wetter floodplains, or possibly the more southerly and easterly location of the Hanna Basin allowed more monsoonal precipitation during the hot PETM summers, particularly if the mountains to the east did not block precipitation. Whatever the ultimate cause, survival of mesic taxa through the CIE body in the Hanna Basin suggests that the extirpations of long-ranging taxa in the BHB resulted from greater water stress and drier floodplains, whereas the brief CIE body appearances of the same tropical palynotaxa in both basins suggests rising temperatures were the major factor in allowing northward range extensions of thermophilic plants.

The climatic affinities of the living relatives of the CIE palynoflora strongly support warming and drying (i.e., the appearance of a dry season and increased water demand) from the Paleocene to the early CIE body. Palms become very abundant during the CIE body (*Arecipites tenuiexinous, A. columellus, Liliacidites tritus, Monocolpollenites tranquillus*), indicating a subtropical to tropical climate (Reichgelt et al., 2018). *A. columellus* is thought to be related to the saw palmetto *Serenoa* (Frederiksen, 1980), a fire-resistant, shrubby, understorey plant currently restricted to the subtropical SE USA (Carrington & Mullahey, 2013; Koptur & Khorsand, 2018). *L. tritus* is thought to be related to *Pseudophoenix*, a genus currently confined to the northern Caribbean islands and coastal areas of mainland North America (Dransfield et al., 2008). These genera are today diverse in dry, subtropical to tropical "prairie" ecosystems (McNab & Edwards, 1980) or inland on dry hills (Dransfield et al., 2008).

Other palynotaxa largely restricted to the CIE body are relatively rare but also show high diversity of living relatives in subtropical or warmer climates. The bean family Fabaceae is represented by *Striatopollis calidarius*, which may belong to the largely tropical tribe Amherstieae (Korasidis et al., 2023; Romero et al., 2020). Fabaceae are also diverse (and abundant) in the megaflora (Wing & Currano, 2013). The palynoflora documents taxa not previously detected in the CIE body, including four types of pollen attributed by Korasidis et al. (2023) to the tribe Bombacoideae in the family Malvaceae (*Bombacadidites* sp., *Friedrichipollis geminus, Retistephanocolporites modicrassus, R. pergrandis*), today a common and diverse group of tropical trees (Zizka et al., 2020). The palynoflora also includes *Brosipollis striata*, belonging to the largely dry tropical family Burseraceae (Espinosa et al., 2006).

Perhaps most surprisingly, given the rarity of ferns in megafloras of the CIE body (Wing & Currano, 2013), fern spores are abundant. *Polypodiaceoisporites gracillimus granoverrucatus* is the most abundant spore type and is probably related to the tropical early successional fern *Pityrogramma* (Korasidis et al., 2023; A. F. Tryon & Lugardon, 2012; R. M. Tryon & Tryon, 2012). *Deltoidospora adriennis* is also common in the CIE body and probably is related to the pantropical "mangrove fern" *Acrostichum aureum* (Jaramillo et al., 2010). *Verrucingulatisporites solox* is thought to be related to the montane tropical fern *Cibotium* (Frederiksen, 1983; R. M. Tryon & Tryon, 2012), and *Azolla cretacea* to tropical floating aquatic ferns in Salviniaceae (Stanley, 1965; R. M. Tryon & Tryon, 2012), which are also present in the megaflora. (*Salvinia* megafossils have long been recognized as an Eocene index in the northern Rockies (Brown, 1948)). *Cicatricosisporites dorogensis* may indicate the presence of the fern *Anemia* (Frederiksen, 1980), which is prolific in the American tropics (R. M. Tryon & Tryon, 2012). The increased abundance of fern spores may represent an increase in the frequency of disturbance, especially during the early part of the CIE body where there is preliminary evidence for the increased density of macro-charcoal particles in the sediment of megafloral sites (Wing et al., 2009). Ferns and charcoal are commonly associated at many fossil sites (McParland et al., 2007 and references therein; Korasidis et al., 2019). The abundance of ferns in the palynoflora suggests they were widespread in the BHB, and the contrast with their rarity in the megaflora may indicate they were more important on distal floodplains than along the margins of the abandoned channels in which megafloras were deposited, though we note the well-known taphonomic bias against the preservation of herbaceous plants with marcescent leaves (Scheihing & Pfefferkorn, 1984). The palynoflora probably gives new insight into the flora of the seasonally dry floodplains of the BHB during the CIE body.

The increased diversity during the CIE body of plants that have high proportions of living relatives in the Af (tropical rainforest) climate types with year-long precipitation and the Am (tropical monsoon) and/or Aw (tropical savanna) climate types, which experience a dry season, is consistent with several lines of evidence for a warmer climate during the CIE body. Fricke and Wing (2004) estimated an increase of ∼5°C from oxygen isotope composition of mammalian tooth enamel, and a similar increase was found in estimates of mean annual temperature from leaf margin analysis (Wing et al., 2005). Paleosol weathering indices and soil nodule geochemistry (Adams et al., 2011; Kraus & Riggins, 2007; Kraus et al., 2013; Woody et al., 2014), accelerated decay rate of soil organic matter (Baczynski et al., 2016, 2019), decreased mammalian body size (Secord et al., 2012), and changes in ichnofossil assemblages (J. J. Smith et al., 2008) are all consistent with major warming and increased seasonality of precipitation.

Subtle differences in palynofloral composition between the NW and SE BHB during the CIE body may also reflect water stress. There is greater diversity of fern spores in the NW BHB, and pollen of some possible xerophytes (e.g., *Brosipollis striata, Chenopodipollis* sp.) is present or more common in the SE BHB. The differences between the NW and SE BHB during the CIE body bear no relationship to time (Figure 10), and the distance between the two areas is only ∼100 km, making it unlikely that the floral differences were the result of regional climate variability. We suggest that water stress was less severe in the northwestern BHB because it was near the structural axis where channels were larger (Foreman, 2014) and floodplain soils were generally coarser (Foreman, 2014; Kraus & Riggins, 2007; Kraus et al., 2013). Paleocurrent directions show that the dominant direction of flow within the BHB was to the north at this time (e.g., Welch et al., 2022). During the CIE body, when temperature, vapor pressure deficit and therefore water demand might have been higher, plants growing on NW BHB floodplains would likely have experienced less water stress because rivers in the NW collected runoff from a larger region and because ground water was more available in the coarser floodplain soils. It is interesting that differences in palynofloral composition between the NW and SE BHB are not seen during the Paleocene, presumably because water stress was less of a factor during cooler periods with more regular rainfall and overall wetter floodplains, even though similar differences in soil grain size and position relative to the basin axis existed.

The importance of water availability to the flora is also suggested by two samples from the latest part of the CIE body in the NW BHB, SLW1515 (PS2202) and SLW1610 (PS1607 & PS1606) that are intermediate in composition between the CIE body and CIE recovery (Figures 5 and 10). Van der Meulen et al. (2020) referred this part of the section to a new faunal subzone, Wa-R, which is characterized by an overlap of typically Wa-0 and Wa-1 mammals. The most prominent paleosol within Wa-R, Purple 4, has features indicating that wetter conditions prevailed at the very end of the CIE body in the NW BHB. It appears that floodplains became wetter again near the end of the CIE body, and that some plants excluded from the BHB by the hotter and more water stressed conditions earlier in the CIE were able to re-establish populations.

During the CIE recovery phase many mesic plant types reappeared that were absent from the CIE body but common during the late Paleocene. These include *Cupressacites hiatipites* (Cupressaceae), *Tricolpites hians* (Platanaceae), three Betulaceae (*Alnipollenites verus, Triporopollenites granilabratus, Triporopollenites infrequens*), and three Juglandaceae (*Caryapollenites veripites, Caryapollenites inelegans, Polyatriopollenites vermontensis*). In the same CIE recovery samples that preserve these mesophytic taxa a few pollen types persist that are otherwise more typical of the CIE body than the Paleocene or later early Eocene: the palms *Arecipites tenuiexinous, Liliacidites tritus,* and *Monocolpollenites tranquillus*, and two eudicots *Aesculiidites circumstriatus* and *Friedrichipollis geminus* (the last is a bombacoid). The persistence of these taxa during the CIE recovery phase may indicate that this period remained warmer than the late Thanetian, even as floodplains became wetter and the carbon isotope composition of the atmosphere increased as the light carbon released during the CIE body was sequestered. The increase in floodplain wetness during the CIE recovery is supported by the continued formation of purplish rather than red paleosols, loss of pedogenic $CaCO_3$ nodules in the SE BHB, and increase in organic-rich sediments (Adams et al., 2011; Baczynski et al., 2013; Kraus & Riggins, 2007; Kraus et al., 2013; van der Meulen et al., 2020; Wing et al., 2009). The CIE recovery also sees the increase in abundance of plants that were not present in the Paleocene, most notably *Platycarya* spp. (Juglandaceae) and *Intratriporopollenites instructus* (Tiliaceae, similar to *Tilia*). *Platycarya* appears to have arrived in North America at the very end of the Paleocene (Frederiksen, 1979, 1980, 1983) or with the onset of the CIE, but was rare in the BHB during the CIE body. *I. instructus* has a first appearance late in the CIE (this paper, Wing et al., 2003). Both taxa likely crossing into North America via high-latitude corridors that had warm, wet climates. The wetter conditions of the CIE recovery also permitted recolonization by mesic species that were extirpated from the BHB during the CIE body, perhaps seeded by populations that had survived the event at higher elevations or in edaphically wetter places (Korasidis et al., 2023; Wing & Currano, 2013). There is direct evidence for refugial populations of mesic species within the Rocky Mountain region in the Hanna Basin (e.g., *Metasequoia* documented by Dechesne et al. (2020)). The regional heterogeneity of environmental stressors during the CIE was probably a major reason for the rapid recolonization of the BHB during the CIE recovery, for the relatively low levels of plant extinction among the high proportion of species that have range gaps during the CIE body, and for the overall compositional similarity of wetland floras in the pre- and post-PETM periods.

Following the end of the CIE recovery phase, early Ypresian palynofloras from the BHB have a high diversity of modern relatives occupying cooler climates and wetter habitats (e.g., *Alnipollenites verus, Sparganiaceaepollenites sp. cf. Sparganium globites, Cupressacites hiatipites*), and palynotaxa with relatives living in tropical or dry tropical climates decline to a minimum for the time interval under study here. The low abundance of *Platycarya* in palynofloras and megafloras during this time, its higher abundance in Wyoming later in the Ypresian during the Early Eocene Climatic Optimum (Wing, 1984), and its abundance in Gulf Coastal Plain palynofloras (Wing & Hickey, 1984), may indicate it preferred warm, wet climates. A cooler and wetter climate during the post-PETM early Ypresian has also been inferred from other proxies including megafloral composition, leaf physiognomy, oxygen isotope composition of hematite nodules, and the common occurrence of tabular carbonaceous shale beds in the central BHB (Bao et al., 1999; Wing, 1984; Wing & Currano, 2013; Wing & Harrington, 2001; Wing et al., 2005, 2009).

The overall pattern of floral change through the PETM in the BHB is consistent with a strong control of composition by climate, probably a combination of temperature and precipitation. This is hardly a surprise given the strong control of plant distributions by climate in the present day. It is more surprising that there were low extinction rates through the large and rapid changes in climate at the onset of the CIE (~5°C warming in ~5 Kyr, globally). Although post-PETM Eocene floras include a substantial number of immigrants, the dominant late Paleocene taxa (e.g., *Cupressacites hiatipites, Alnipollenites verus, Polyatriopollenites vermontensis, Triporopollenites granilabratus,* and *T. infrequens*) are still common in the same wet floodplain settings they occupied prior to the PETM. This persistence is clearly not the result of an ecological-timescale incumbency, since both the taxa and the habitats they occupied were absent from the BHB for 100 ka. It is much better explained by the combination of a relatively constant regional species pool in the absence of high extinction, and conservative niche preferences among the regional pool of wetland plant species (DiMichele et al., 2004; Prinzing et al., 2001). Without sample spacing at an ecological timescale (i.e., millennial) it is difficult to know if the individual taxa occupying the wet floodplain habitat return to the BHB en masse, as would be predicted if their co-occurrence depends on a few common environmental variables, or if there are some taxa that return more quickly than others.

A final somewhat unexpected result of this work is that we detected no significant change in palynofloral richness or taxon abundance distributions across the PETM at any spatial scale from within sample to pooled time bins (Tables 1 and 2; Figure 7). The notable shift in floral composition, consistent with a change from warm-temperate

to dry-tropical forest and back again, might have been expected to correspond to a temporary increase in diversity associated with the arrival of a warmer climate because of the higher diversity of tropical vegetation and palynofloras (e.g., Gosling et al., 2018). The relatively constant diversity in the palynoflora could be real, that is, the appearance of "PETM only" species approximately offset the disappearance of "PETM range gap" species, leading to no net change. It is also possible that the massive change in climate, which likely affected pollen production, transport, and preservation, has made changes in diversity hard to detect. As discussed above, the alternating wet/dry floodplains of the CIE body would have reduced pollen preservation (Havinga, 1964), with the result that pollen assemblages preserved in abandoned channels contain mostly grains deposited directly into the pond, with little admixture of grains reworked from geologically short-term storage in wet floodplain soils. The palynofloras preserved during the CIE body within abandoned channel fills and in-channel mud drapes, were likely preserved via rapid burial. As a result of these processes, individual samples from the CIE body may represent less time and space than samples from earlier and later times, even those that come from the same depositional environments. More work is needed to understand the possibly opposing influences that climate change might have had on taphonomic processes and floral diversity.

5. Conclusions

1. There was a rapid, basin-wide change in floral composition within an ∼30 ka period that includes the onset of the negative CIE associated with the PETM. The changes in composition are consistent with extirpation of warm-temperate to subtropical mesic plants and their replacement by tropical plants, some of which were likely tolerant of seasonal water stress. The earliest PETM palynofloras may indicate a phase during which vegetation was frequently disturbed and dominated by ferns and palms.
2. Changes in floral composition during the last ∼40 ka of the Paleocene suggest warming and drying were underway prior to the PETM, probably coincident with small carbon isotope excursions prior to the main CIE.
3. The composition of CIE-recovery floras indicates a period during which temperatures were still elevated above those of the late Paleocene, but floodplain wetness had increased once again.
4. Post-PETM early Eocene floras include a few immigrant taxa that likely arrived in North America via high-latitude land bridges, but most taxa important in wet Paleocene floodplain floras remained important in the Eocene.
5. These rapid, climatically forced changes in floral composition took place without major extinction, perhaps indicating that there were nearby refugia in which plants adapted to wetter substrates and/or cooler climates could persist.
6. Although reworking of organic microfossils increased during the PETM because of rapid erosion of Paleocene and Cretaceous mud rocks around the margins of the BHB, large changes in palynofloral composition remain visible, though the degree and rate of change is better represented if reworked grains are excluded from analysis.
7. Overall, the palynofloral record is consistent with megaflora, isotopic and paleosol evidence that rapid increases in water stress and temperature during the PETM forced basin-wide extirpation of some plants and permitted immigration of more thermophilic and drought tolerant lineages from other regions, but was not sufficient to cause extinction and diversity loss.

Data Availability Statement

The data and R code that support the findings of this study are openly available in Figshare via Korasidis and Wing (2023a), Korasidis and Wing (2023b), Korasidis and Wing (2023c), Korasidis and Wing (2023d), Korasidis and Wing (2023e), and Korasidis and Wing (2023f).

Acknowledgments
Funding for this research was provided through a Smithsonian Institution Peter Buck Postdoctoral Fellowship Award to VAK. VAK is currently funded through an Elizabeth and Vernon Puzey Fellowship Award. SLW fieldwork was supported by the Roland W. Brown fund of the Dept. of Paleobiology, and by the MacMillan Fund of the NMNH. We thank Philip D. Gingerich and Hemmo Abels for many conversations about the litho- and biostratigraphy of the NW BHB, and for their guidance in the field. Jon Bloch, Paul Morse, Doug Boyer, Mary Kraus, and Tom Bown provided similar help in the SE BHB. We thank Brady Foreman for conversations about fluvial landscapes and temporal resolution in the Paleocene-Eocene sequences of the BHB, and Kay Behrensmeyer for conversations about taphonomy and depositional environments. We also thank Guy Harrington for assistance with palynofloral identification. We greatly appreciate the long-time support and friendship of the Churchill family of Powell, Wyoming, and the showers and other hospitality of Holly Smith and Philip Gingerich. Open access publishing facilitated by The University of Melbourne, as part of the Wiley - The University of Melbourne agreement via the Council of Australian University Librarians.

References

Abels, H. A., Kraus, M. J., & Gingerich, P. D. (2013). Precession-scale cyclicity in the fluvial lower Eocene Willwood Formation of the Bighorn Basin, Wyoming (USA). *Sedimentology*, *60*(6), 1467–1483. https://doi.org/10.1111/sed.12039

Adams, J. S., Kraus, M. J., & Wing, S. L. (2011). Evaluating the use of weathering indices for determining mean annual precipitation in the ancient stratigraphic record. *Palaeogeography, Palaeoclimatology, Palaeoecology*, *309*(3–4), 358–366. https://doi.org/10.1016/j.palaeo.2011.07.004

Averyanov, L. V., Phan, K. L., Nguyen, T. H., Nguyen, S. K., Nguyen, T. V., & Pham, T. D. (2009). Preliminary observation of native *Glyptostrobus pensilis* (Taxodiaceae) stands in Vietnam. *Taiwania*, *54*(3), 191–212.

Azevedo-Schmidt, L., Diefendorf, A. F., Schlanser, K., Baczynski, A. A., Dechesne, M., Dunn, R., et al. (2022). Local differences in paleohydrology have stronger influence on plant biomarkers than regional climate change across two Paleogene Laramide Basins, Wyoming, USA. *Palaeogeography, Palaeoclimatology, Palaeoecology*, *596*, 110977. https://doi.org/10.1016/j.palaeo.2022.110977

Aziz, H. A., Hilgen, F. J., van Luijk, G. M., Sluijs, A., Kraus, M. J., Pares, J. M., & Gingerich, P. D. (2008). Astronomical climate control on paleosol stacking patterns in the upper Paleocene–lower Eocene Willwood Formation, Bighorn Basin, Wyoming. *Geology*, *36*(7), 531–534. https://doi.org/10.1130/G24734A.1

Baczynski, A. A., McInerney, F. A., Freeman, K. H., Wing, S. L., & Bighorn Basin Coring Project (BBCP) Science Team. (2019). Carbon isotope record of trace n-alkanes in a continental PETM section recovered by the Bighorn Basin Coring Project (BBCP). *Paleoceanography and Paleoclimatology*, *34*(5), 853–865. https://doi.org/10.1029/2019PA003579

Baczynski, A. A., McInerney, F. A., Wing, S. L., Kraus, M. J., Bloch, J. I., Boyer, D. M., et al. (2013). Chemostratigraphic implications of spatial variation in the Paleocene-Eocene Thermal Maximum carbon isotope excursion, SE Bighorn Basin, Wyoming. *Geochemistry, Geophysics, Geosystems*, *14*(10), 4133–4152. https://doi.org/10.1002/ggge.20265

Baczynski, A. A., McInerney, F. A., Wing, S. L., Kraus, M. J., Morse, P. E., Bloch, J. I., et al. (2016). Distortion of carbon isotope excursion in bulk soil organic matter during the Paleocene-Eocene thermal maximum. *GSA Bulletin*, *128*(9–10), 1352–1366. https://doi.org/10.1130/B31389.1

Bao, H., Koch, P. L., & Rumble, III, D. (1999). Paleocene–Eocene climatic variation in western North America: Evidence from the $\delta^{18}O$ of pedogenic hematite. *Geological Society of America Bulletin*, *111*(9), 1405–1415. https://doi.org/10.1130/0016-7606(1999)111<1405:PECVIW>2.3.CO;2

Beck, H. E., Zimmermann, N. E., McVicar, T. R., Vergopolan, N., Berg, A., & Wood, E. F. (2018). Present and future Köppen-Geiger climate classification maps at 1-km resolution. *Scientific Data*, *5*(1), 1–12. https://doi.org/10.1038/sdata.2018.214

Betts, R. A., Boucher, O., Collins, M., Cox, P. M., Falloon, P. D., Gedney, N., et al. (2007). Projected increase in continental runoff due to plant responses to increasing carbon dioxide. *Nature*, *448*(7157), 1037–1041. https://doi.org/10.1038/nature06045

Bowen, G. J., Bralower, T. J., Delaney, M. L., Dickens, G. R., Kelly, D. C., Koch, P. L., et al. (2006). Eocene hyperthermal event offers insight into greenhouse warming. *Eos, Transactions American Geophysical Union*, *87*(17), 165–169. https://doi.org/10.1029/2006eo170002

Bowen, G. J., Koch, P. L., Gingerich, P. D., Norris, R. D., Bains, S., & Corfield, R. M. (2001). Refined isotope stratigraphy across the continental Paleocene-Eocene boundary on Polecat Bench in the northern Bighorn Basin: Paleocene-Eocene Stratigraphy and Biotic Change in the Bighorn and Clarks Fork Basins, Wyoming. *University of Michigan Papers on Paleontology*, *33*, 73–88.

Bowen, G. J., Maibauer, B. J., Kraus, M. J., Röhl, U., Westerhold, T., Steimke, A., et al. (2015). Two massive, rapid releases of carbon during the onset of the Palaeocene–Eocene Thermal Maximum. *Nature Geoscience*, *8*(1), 44–47. https://doi.org/10.1038/ngeo2316

Bown, T. M. (1980). Summary of latest Cretaceous and Cenozoic sedimentary, tectonic, and erosional events, Bighorn Basin, Wyoming. In *Early Cenozoic paleontology and stratigraphy of the Bighorn Basin, Wyoming* (Vol. 24, pp. 25–32). University of Michigan Papers on Paleontology.

Bown, T. M., Holroyd, P. A., & Rose, K. D. (1994). Mammal extinctions, body size, and paleotemperature. *Proceedings of the National Academy of Sciences*, *91*(22), 10403–10406. https://doi.org/10.1073/pnas.91.22.10403

Bown, T. M., & Kraus, M. J. (1981). Lower Eocene alluvial paleosols (Willwood Formation, northwest Wyoming, USA) and their significance for paleoecology, paleoclimatology, and basin analysis. *Palaeogeography, Palaeoclimatology, Palaeoecology*, *34*, 1–30. https://doi.org/10.1016/0031-0182(81)90056-0

Brown, R. W. (1948). Age of the Kingsbury conglomerate is Eocene. *Geological Society of America Bulletin*, *59*(11), 1165–1172. https://doi.org/10.1130/0016-7606(1948)59[1165:aotkci]2.0.co;2

Carmichael, M. J., Inglis, G. N., Badger, M. P., Naafs, B. D. A., Behrooz, L., Remmelzwaal, S., et al. (2017). Hydrological and associated biogeochemical consequences of rapid global warming during the Paleocene-Eocene Thermal Maximum. *Global and Planetary Change*, *157*, 114–138. https://doi.org/10.1016/j.gloplacha.2017.07.014

Carmichael, M. J., Pancost, R. D., & Lunt, D. J. (2018). Changes in the occurrence of extreme precipitation events at the Paleocene–Eocene thermal maximum. *Earth and Planetary Science Letters*, *501*, 24–36. https://doi.org/10.1016/j.epsl.2018.08.005

Carrington, M. E., & Mullahey, J. J. (2013). Saw palmetto (*Serenoa repens*) flowering and fruiting response to time since fire. *Rangeland Ecology & Management*, *66*(1), 43–50. https://doi.org/10.2111/REM-D-11-00183.1

Clyde, W. C., & Gingerich, P. D. (1998). Mammalian community response to the latest Paleocene thermal maximum: An isotaphonomic study in the northern Bighorn Basin, Wyoming. *Geology*, *26*(11), 1011–1014. https://doi.org/10.1130/0091-7613(1998)026<1011:mcrttl>2.3.co;2

Clyde, W. C., Gingerich, P. D., Wing, S. L., Röhl, U., Westerhold, T., Bowen, G., et al. (2013). Bighorn Basin Coring Project (BBCP): A continental perspective on early Paleogene hyperthermals. *Scientific Drilling*, *16*, 21–31. https://doi.org/10.5194/sd-16-21-2013

Clyde, W. C., Hamzi, W., Finarelli, J. A., Wing, S. L., Schankler, D., & Chew, A. (2007). Basin-wide magnetostratigraphic framework for the Bighorn Basin, Wyoming. *Geological Society of America Bulletin*, *119*(7–8), 848–859. https://doi.org/10.1130/B26104.1

Cramwinckel, M. J., Huber, M., Kocken, I. J., Agnini, C., Bijl, P. K., Bohaty, S. M., et al. (2018). Synchronous tropical and polar temperature evolution in the Eocene. *Nature*, *559*(7714), 382–386. https://doi.org/10.1038/s41586-018-0272-2

Currano, E. D., Wilf, P., Wing, S. L., Labandeira, C. C., Lovelock, E. C., & Royer, D. L. (2008). Sharply increased insect herbivory during the Paleocene–Eocene Thermal Maximum. *Proceedings of the National Academy of Sciences*, *105*(6), 1960–1964. https://doi.org/10.1073/pnas.0708646105

Davies-Vollum, K. S. (2001). Not just red beds: The occurrence and formation of drab sections in the Willwood Formation of the Bighorn Basin. In P. D. Gingerich (Ed.), *Paleocene-Eocene stratigraphy and biotic change in the Bighorn and Clarks Fork basins, Wyoming* (Vol. 33, pp. 29–35). University of Michigan Papers on Paleontology.

Davies-Vollum, S. K., & Wing, S. L. (1998). Sedimentological, taphonomic, and climatic aspects of Eocene swamp deposits (Willwood Formation, Bighorn Basin, Wyoming). *Palaios*, *13*(1), 28–40. https://doi.org/10.2307/3515279

Dechesne, M., Currano, E. D., Dunn, R. E., Higgins, P., Hartman, J. H., Chamberlain, K. R., & Holm-Denoma, C. S. (2020). A new stratigraphic framework and constraints for the position of the Paleocene–Eocene boundary in the rapidly subsiding Hanna Basin, Wyoming. *Geosphere*, *16*(2), 594–618. https://doi.org/10.1130/GES02118.1

Denk, T., Grimm, G. W., Grímsson, F., & Zetter, R. (2013). Evidence from "Köppen signatures" of fossil plant assemblages for effective heat transport of Gulf Stream to subarctic North Atlantic during Miocene cooling. *Biogeosciences*, *10*(12), 7927–7942. https://doi.org/10.5194/bg-10-7927-2013

Denk, T., & Tekleva, M. V. (2006). Comparative pollen morphology and ultrastructure of *Platanus*: Implications for phylogeny and evaluation of the fossil record. *Grana*, *45*(3), 195–221. https://doi.org/10.1080/00173130600873901

DiMichele, W. A., Behrensmeyer, A. K., Olszewski, T. D., Labandeira, C. C., Pandolfi, J. M., Wing, S. L., & Bobe, R. (2004). Long-term stasis in ecological assemblages: Evidence from the fossil record. *Annual Reviews of Ecolology, Evolution and Systematics*, *35*(1), 285–322. https://doi.org/10.1146/annurev.ecolsys.35.120202.110110

Drake, B. G., Gonzàlez-Meler, M. A., & Long, S. P. (1997). More efficient plants: A consequence of rising atmospheric CO_2? *Annual Review of Plant Biology*, *48*(1), 609–639. https://doi.org/10.1146/annurev.arplant.48.1.609

Dransfield, J., Uhl, N. W., Asmussen, C. B., Baker, W. J., Harley, M. M., & Lewis, C. E. (2008). *Genera Palmarum: The Evolution and Classification of the Palms*. Key Publishing, Royal Botanical Gardens.

Dunkley Jones, T., Ridgwell, A., Lunt, D. J., Maslin, M. A., Schmidt, D. N., & Valdes, P. J. (2010). A Palaeogene perspective on climate sensitivity and methane hydrate instability. *Philosophical Transactions of the Royal Society A: Mathematical, Physical & Engineering Sciences*, *368*(1919), 2395–2415. https://doi.org/10.1098/rsta.2010.0053

Dunkley Jones, T. D., Lunt, D. J., Schmidt, D. N., Ridgwell, A., Sluijs, A., Valdes, P. J., & Maslin, M. (2013). Climate model and proxy data constraints on ocean warming across the Paleocene–Eocene Thermal Maximum. *Earth-Science Reviews*, *125*, 123–145. https://doi.org/10.1016/j.earscirev.2013.07.004

Elsik, W. C. (1968). *Palynology of a Paleocene Rockdale lignite, Milam County, Texas. Part II. Morphology and Taxonomy* (pp. 599–664). Muséum National d'Histoire Naturelle.

Espinosa, D., Llorente, J., & Morrone, J. J. (2006). Historical biogeographical patterns of the species of *Bursera* (Burseraceae) and their taxonomic implications. *Journal of Biogeography*, *33*(11), 1945–1958. https://doi.org/10.1111/j.1365-2699.2006.01566.x

Farley, M. B. (1989). Palynological facies fossils in nonmarine environments in the Paleogene of the Bighorn Basin. *Palaios*, *4*(6), 565–573. https://doi.org/10.2307/3514746

Farley, M. B. (1990). Vegetation distribution across the Early Eocene depositional landscape from palynological analysis. *Palaeogeography, Palaeoclimatology, Palaeoecology*, *79*(1–2), 11–27. https://doi.org/10.1016/0031-0182(90)90103-e

Feng, Y., Oh, S. H., & Manos, P. S. (2005). Phylogeny and historical biogeography of the genus Platanus as inferred from nuclear and chloroplast DNA. *Systematic Botany*, *30*(4), 786–799. https://doi.org/10.1600/036364405775097851

Foreman, B., Heller, P., & Clementz, M. (2012). Fluvial response to abrupt global warming at the Palaeocene/Eocene boundary. *Nature*, *491*(7422), 92–95. https://doi.org/10.1038/nature11513

Foreman, B. Z. (2014). Climate-driven generation of a fluvial sheet sand body at the Paleocene–Eocene boundary in north-west Wyoming (USA). *Basin Research*, *26*(2), 225–241. https://doi.org/10.1111/bre.12027

Foreman, B. Z., & Straub, K. M. (2017). Autogenic geomorphic processes determine the resolution and fidelity of terrestrial paleoclimate records. *Science Advances*, *3*(9), e1700683. https://doi.org/10.1126/sciadv.1700683

Fragnière, Y., Song, Y. G., Fazan, L., Manchester, S. R., Garfì, G., & Kozlowski, G. (2021). Biogeographic overview of Ulmaceae: Diversity, distribution, ecological preferences, and conservation status. *Plants*, *10*(6), 1111. https://doi.org/10.3390/plants10061111

Frederiksen, N. O. (1979). Paleogene sporomorph biostratigraphy, northeastern Virginia. *Palynology*, *3*(1), 129–167. https://doi.org/10.1080/01916122.1979.9989187

Frederiksen, N. O. (1980). Paleogene sporomorphs from South Carolina and quantitative correlations with the Gulf Coast. *Palynology*, *4*(1), 125–179. https://doi.org/10.1080/01916122.1980.9989205

Frederiksen, N. O. (1983). Late Paleocene and early Eocene sporomorphs and thermal alteration of organic matter in the Santa Susana Formation, southern California. In R. R. Squires & M. V. Filewin (Eds.), *Cenozoic geology of the Simi Valley area, southern California: Pacific Section, Society of Economic Paleontologists and Mineralogists, fall field trip volume and guidebook* (pp. 23–31).

Fricke, H. C., Clyde, W. C., O'Neil, J. R., & Gingerich, P. D. (1998). Evidence for rapid climate change in North America during the latest Paleocene thermal maximum: Oxygen isotope compositions of biogenic phosphate from the Bighorn Basin (Wyoming). *Earth and Planetary Science Letters*, *160*(1–2), 193–208. https://doi.org/10.1016/s0012-821x(98)00088-0

Fricke, H. C., & Wing, S. L. (2004). Oxygen isotope and paleobotanical estimates of temperature and $\delta^{18}O$–latitude gradients over North America during the early Eocene. *American Journal of Science*, *304*(7), 612–635. https://doi.org/10.2475/ajs.304.7.612

Furlow, J. J. (1979). The systematics of the American species of *Alnus* (Betulaceae). *Rhodora*, *81*(825), 1–121.

Gingerich, P. D. (1989). *New earliest Wasatchian mammalian fauna from the Eocene of northwestern Wyoming: Composition and diversity in a rarely sampled high-floodplain assemblage* (Vol. 28, pp. 1–97). University of Michigan Papers on Paleontology.

Gingerich, P. D. (2001). *Biostratigraphy of the continental Paleocene-Eocene boundary interval on Polecat Bench in the northern Bighorn Basin. Paleocene–Eocene Stratigraphy and Biotic Change in the Bighorn and Clarks Fork Basins, Wyoming* (Vol. 33, pp. 37–67). University of Michigan Papers on Paleontology.

Gingerich, P. D. (2003). Mammalian responses to climate change at the Paleocene-Eocene boundary: Polecat Bench. In S. Wing (Ed.), *Causes and consequences of globally warm climates in the early Paleogene* (Vol. 369, pp. 463–478). Geological Society of America Special Papers.

Gingerich, P. D., & Clyde, W. C. (2001). *Overview of mammalian biostratigraphy in the Paleocene-Eocene Fort Union and Willwood formations of the Bighorn and Clarks Fork basins* (Vol. 33, pp. 1–14). University of Michigan Papers on Paleontology.

Gingerich, P. D., & Smith, T. (2006). Paleocene-Eocene land mammals from three new latest Clarkforkian and earliest Wasatchian wash sites at Polecat Bench in the northern Bighorn Basin, Wyoming.

Gosling, W. D., Julier, A. C., Adu-Bredu, S., Djagbletey, G. D., Fraser, W. T., Jardine, P. E., et al. (2018). Pollen-vegetation richness and diversity relationships in the tropics. *Vegetation History and Archaeobotany*, *27*(2), 411–418. https://doi.org/10.1007/s00334-017-0642-y

Greenwood, D. R., Archibald, S. B., Mathewes, R. W., & Moss, P. T. (2005). Fossil biotas from the Okanagan Highlands, southern British Columbia and northeastern Washington State: Climates and ecosystems across an Eocene landscape. *Canadian Journal of Earth Sciences*, *42*(2), 167–185. https://doi.org/10.1139/e04-100

Gutjahr, M., Ridgwell, A., Sexton, P. F., Anagnostou, E., Pearson, P. N., Pälike, H., et al. (2017). Very large release of mostly volcanic carbon during the Palaeocene–Eocene Thermal Maximum. *Nature*, *548*(7669), 573–577. https://doi.org/10.1038/nature23646

Harrington, G. J. (2001). *Pollen assemblages and Paleocene-Eocene stratigraphy in the Bighorn and Clarks Fork Basins* (Vol. 33, pp. 89–96). University of Michigan Papers on Paleontology.

Havinga, A. J. (1964). Investigation into the differential corrosion susceptibility of pollen and spores. *Pollen et Spores*, *4*, 621–635.

Haynes, L. L., & Hönisch, B. (2020). The seawater carbon inventory at the Paleocene–Eocene Thermal Maximum. *Proceedings of the National Academy of Sciences*, *117*(39), 24088–24095. https://doi.org/10.1073/pnas.2003197117

Inglis, G. N., Bragg, F., Burls, N. J., Cramwinckel, M. J., Evans, D., Foster, G. L., et al. (2020). Global mean surface temperature and climate sensitivity of the early Eocene Climatic Optimum (EECO), Paleocene–Eocene Thermal Maximum (PETM), and latest Paleocene. *Climate of the Past*, *16*(5), 1953–1968. https://doi.org/10.5194/cp-16-1953-2020

Jacobson, G. L., & Bradshaw, R. H. (1981). The Selection of Sites for Paleovegetational Studies 1. *Quaternary Research*, *16*(1), 80–96. https://doi.org/10.1016/0033-5894(81)90129-0

Jaramillo, C., Ochoa, D., Contreras, L., Pagani, M., Carvajal-Ortiz, H., Pratt, L. M., et al. (2010). Effects of rapid global warming at the Paleocene–Eocene boundary on neotropical vegetation. *Science*, *330*(6006), 957–961. https://doi.org/10.1126/science.1193833

Jerolmack, D. J., & Sadler, P. (2007). Transience and persistence in the depositional record of continental margins. *Journal of Geophysical Research*, *112*(F3), F03S13. https://doi.org/10.1029/2006JF000555

Jones, T. D., Lunt, D. J., Schmidt, D. N., Ridgwell, A., Sluijs, A., Valdes, P. J., & Maslin, M. (2013). Climate model and proxy data constraints on ocean warming across the Paleocene–Eocene Thermal Maximum. *Earth-Science Reviews*, *125*, 123–145. https://doi.org/10.1016/j.earscirev.2013.07.004

Kennett, J. P., & Stott, L. D. (1991). Abrupt deep-sea warming, palaeoceanographic changes and benthic extinctions at the end of the Palaeocene. *Nature*, *353*(6341), 225–229. https://doi.org/10.1038/353225a0

Koch, P. L., Zachos, J. C., & Gingerich, P. D. (1992). Correlation between isotope records in marine and continental carbon reservoirs near the Palaeocene/Eocene boundary. *Nature*, *358*(6384), 319–322. https://doi.org/10.1038/358319a0

Köppen, W., & Geiger, R. (1936). *Das geographische System der Klimate* (p. 44). Borntraeger.

Koptur, S., & Khorsand, R. (2018). Pollination ecology of three sympatric palms of southern Florida pine rocklands. *Natural Areas Journal*, *38*(1), 15–25. https://doi.org/10.3375/043.038.0104

Korasidis, V. A., Wallace, M. W., Wagstaff, B. E., & Hill, R. S. (2019). Evidence of fire in Australian Cenozoic rainforests. *Palaeogeography, Palaeoclimatology, Palaeoecology*, *516*, 35–43. https://doi.org/10.1016/j.palaeo.2018.11.023

Korasidis, V. A., & Wing, S. L. (2023a). Table S1 [Dataset]. University of Melbourne. https://doi.org/10.26188/24530449.v2

Korasidis, V. A., & Wing, S. L. (2023b). Table S2 [Dataset]. University of Melbourne. https://doi.org/10.26188/24530485.v2

Korasidis, V. A., & Wing, S. L. (2023c). Table S3 [Dataset]. University of Melbourne. https://doi.org/10.26188/24530497.v3

Korasidis, V. A., & Wing, S. L. (2023d). Table S4 [Dataset]. University of Melbourne. https://doi.org/10.26188/24530512.v2

Korasidis, V. A., & Wing, S. L. (2023e). Table S5 [Dataset]. University of Melbourne. https://doi.org/10.26188/24530527.v2

Korasidis, V. A., & Wing, S. L. (2023f). Text S1 [Software]. University of Melbourne. https://doi.org/10.26188/24539401.v1

Korasidis, V. A., Wing, S. L., Harrington, G., Demchuk, T., Gravendyck, J., Jardine, P. E., & Willard, D. (2023). New and important biostratigraphic palynofloras from the Paleocene–Eocene boundary of North America. *Palynology*, *47*(1), 2115159. https://doi.org/10.1080/01916122.2022.2115159

Korasidis, V. A., Wing, S. L., Nelson, D. M., & Baczynski, A. A. (2022). Reworked pollen reduces apparent floral change during the Paleocene-Eocene Thermal Maximum. *Geology*, *50*(12), 1398–1402. https://doi.org/10.1130/G50441.1

Korasidis, V. A., Wing, S. L., Shields, C. A., & Kiehl, J. T. (2022). Global changes in terrestrial vegetation and continental climate during the Paleocene-Eocene Thermal Maximum. *Paleoceanography and Paleoclimatology*, *37*(4), e2021PA004325. https://doi.org/10.1029/2021PA004325

Kottek, M., Grieser, J., Beck, C., Rudolf, B., & Rubel, F. (2006). World map of the Köppen-Geiger climate classification updated.

Kozdon, R., Kelly, D. C., Kitajima, K., Strickland, A., Fournelle, J. H., & Valley, J. W. (2013). In situ $\delta^{18}O$ and Mg/Ca analyses of diagenetic and planktic foraminiferal calcite preserved in a deep-sea record of the Paleocene-Eocene thermal maximum. *Paleoceanography*, *28*(3), 517–528. https://doi.org/10.1002/palo.20048

Kozlowski, G., Song, Y. G., Bétrisey, S., Alvarado, E. V., & Bétrisey, S. (2018). *Wingnuts (" Pterocarya") & walnut family: Relict trees: Linking the past, present and future*. Natural History Museum.

Kraus, M. J., McInerney, F. A., Wing, S. L., Secord, R., Baczynski, A. A., & Bloch, J. I. (2013). Paleohydrologic response to continental warming during the Paleocene–Eocene thermal maximum, Bighorn Basin, Wyoming. *Palaeogeography, Palaeoclimatology, Palaeoecology*, *370*, 196–208. https://doi.org/10.1016/j.palaeo.2012.12.008

Kraus, M. J., & Riggins, S. (2007). Transient drying during the Paleocene–Eocene Thermal Maximum (PETM): Analysis of paleosols in the Bighorn Basin, Wyoming. *Palaeogeography, Palaeoclimatology, Palaeoecology*, *245*(3–4), 444–461. https://doi.org/10.1016/j.palaeo.2006.09.011

Kraus, M. J., Woody, D. T., Smith, J. J., & Dukic, V. (2015). Alluvial response to the Paleocene–Eocene thermal maximum climatic event, polecat bench, Wyoming (USA). *Palaeogeography, Palaeoclimatology, Palaeoecology*, *435*, 177–192. https://doi.org/10.1016/j.palaeo.2015.06.021

Li, M., Bralower, T. J., Kump, L. R., Self-Trail, J. M., Zachos, J. C., Rush, W. D., & Robinson, M. M. (2022). Astrochronology of the Paleocene-Eocene Thermal Maximum on the Atlantic Coastal Plain. *Nature Communications*, *13*(1), 5618. https://doi.org/10.1038/s41467-022-33390-x

Love, J. D., & Christiansen, A. C. (1985). *Geologic map of Wyoming*. US Geological Survey.

Magioncalda, R., Dupuis, C., Smith, T., Steurbaut, E., & Gingerich, P. D. (2004). Paleocene-Eocene carbon isotope excursion in organic carbon and pedogenic carbonate: Direct comparison in a continental stratigraphic section. *Geology*, *32*(7), 553–556. https://doi.org/10.1130/G20476.1

Manchester, S. R. (1986). Vegetative and reproductive morphology of an extinct plane tree (Platanaceae) from the Eocene of western North America. *Botanical Gazette*, *147*(2), 200–226. https://doi.org/10.1086/337587

Manchester, S. R., & Dilcher, D. L. (1997). Reproductive and vegetative morphology of *Polyptera* (Juglandaceae) from the Paleocene of Wyoming and Montana. *American Journal of Botany*, *84*(5), 649–663. https://doi.org/10.2307/2445902

Manchester, S. R., Pigg, K. B., & Crane, P. R. (2004). *Palaeocarpinus dakotensis* sp. n. (Betulaceae: Coryloideae) and associated staminate catkins, pollen, and leaves from the Paleocene of North Dakota. *International Journal of Plant Sciences*, *165*(6), 1135–1148. https://doi.org/10.1086/423870

Marchin, R. M., Medlyn, B. E., Tjoelker, M. G., & Ellsworth, D. S. (2023). Decoupling between stomatal conductance and photosynthesis occurs under extreme heat in broadleaf tree species regardless of water access. *Global Change Biology*, *29*(22), 6319–6335. https://doi.org/10.1111/gcb.16929

McInerney, F. A., & Wing, S. L. (2011). The Paleocene-Eocene Thermal Maximum: A perturbation of carbon cycle, climate, and biosphere with implications for the future. *Annual Review of Earth and Planetary Sciences*, *39*(1), 489–516. https://doi.org/10.1146/annurev-earth-040610-133431

McNab, W. H., & Edwards, M. B., Jr. (1980). Climatic factors related to the range of saw-palmetto (Serenoa repens (Bartr.) Small). *The American Midland Naturalist*, *103*(1), 204–208. https://doi.org/10.2307/2425058

McParland, L. C., Collinson, M. E., Scott, A. C., Steart, D. C., Grassineau, N. V., & Gibbons, S. J. (2007). Ferns and fires: Experimental charring of ferns compared to wood and implications for paleobiology, paleoecology, coal petrology, and isotope geochemistry. *Palaios*, *22*(5), 528–538. https://doi.org/10.2110/palo.2005.p05-138r

Murphy, B. H., Farley, K. A., & Zachos, J. C. (2010). An extraterrestrial ^{3}He-based timescale for the Paleocene–Eocene thermal maximum (PETM) from Walvis Ridge, IODP Site 1266. *Geochimica et Cosmochimica Acta*, *74*(17), 5098–5108. https://doi.org/10.1016/j.gca.2010.03.039

Neasham, J. W., & Vondra, C. F. (1972). Stratigraphy and petrology of the lower Eocene Willwood formation, Bighorn Basin, Wyoming. *Geological Society of America Bulletin*, *83*(7), 2167–2180. https://doi.org/10.1130/0016-7606(1972)83[2167:sapotl]2.0.co;2

Nichols, D. J. (2010). *Reevaluation of the holotypes of the Wodehouse pollen species from the Green River Formation (Eocene, Colorado and Utah)*. American Association of Stratigraphic Palynologists Foundation.

Nichols, D. J., & Brown, J. L. (1992). Palynostratigraphy of the Tullock Member (lower Paleocene) of the Fort Union Formation in the Powder River Basin, Montana and Wyoming. *United States Geological Survey Bulletin*, *1917*, 1–35.

Nixon, K. C., & Poole, J. M. (2003). Revision of the Mexican and Guatemalan species of *Platanus* (Platanaceae). *Lundellia*, *6*(1), 103–137. https://doi.org/10.25224/1097-993X-6.1.4

Peppe, D. J., Baumgartner, A., Flynn, A., & Blonder, B. (2018). Reconstructing Paleoclimate and Paleoecology Using Fossil Leaves. In D. Croft, D. Su, & S. Simpson (Eds.), *Methods in Paleoecology. Vertebrate Paleobiology and Paleoanthropology*. Springer. https://doi.org/10.1007/978-3-319-94265-0_13

Pezzini, F. F., Dexter, K. G., de Carvalho-Sobrinho, J. G., Kidner, C. A., Nicholls, J. A., De Queiroz, L. P., & Pennington, R. T. (2021). Phylogeny and biogeography of *Ceiba* Mill. (Malvaceae, Bombacoideae). *Frontiers of Biogeography*, *13*(2), e49226. https://doi.org/10.1101/2020.07.10.196238

Pocknall, D. T. (1987). Palynomorph biozones for the fort Union and Wasatch formations (upper Paleocene–lower Eocene), Powder River Basin, Wyoming and Montana, USA. *Palynology*, *11*(1), 23–35. https://doi.org/10.1080/01916122.1987.9989316

Pocknall, D. T., & Nichols, D. J. (1996). Palynology of coal zones of the Tongue River Member (Upper Paleocene) of the Fort Union Formation, Powder River Basin, Montana and Wyoming. *American Association of Stratigraphic Palynology Contribution Series*, *32*, 1–58.

Prinzing, A., Durka, W., Klotz, S., & Brandl, R. (2001). The niche of higher plants: Evidence for phylogenetic conservatism. *Proceedings of the Royal Society of London. Series B: Biological Sciences*, *268*(1483), 2383–2389. https://doi.org/10.1098/rspb.2001.1801

Ramos, E. J., Breecker, D. O., Barnes, J. D., Li, F., Gingerich, P. D., Loewy, S. L., et al. (2022). Swift weathering response on floodplains during the Paleocene-Eocene Thermal Maximum. *Geophysical Research Letters*, *49*(6), e2021GL097436. https://doi.org/10.1029/2021GL097436

R Core Team. (2022). *RStudio*. Integrated Development for R. RStudio, PBC.

Reichgelt, T., West, C. K., & Greenwood, D. R. (2018). The relation between global palm distribution and climate. *Scientific Reports*, *8*(1), 1–11. https://doi.org/10.1038/s41598-018-23147-2

Röhl, U., Westerhold, T., Bralower, T. J., & Zachos, J. C. (2007). On the duration of the Paleocene-Eocene thermal maximum (PETM). *Geochemistry, Geophysics, Geosystems*, *8*(12). https://doi.org/10.1029/2007GC001784

Romero, I. C., Kong, S., Fowlkes, C. C., Jaramillo, C., Urban, M. A., Oboh-Ikuenobe, F., et al. (2020). Improving the taxonomy of fossil pollen using convolutional neural networks and superresolution microscopy. *Proceedings of the National Academy of Sciences*, *117*(45), 28496–28505. https://doi.org/10.1073/pnas.2007324117

Rose, K. D., Chew, A. E., Dunn, R. H., Kraus, M. J., Fricke, H. C., & Zack, S. P. (2012). *Earliest Eocene mammalian fauna from the Paleocene-Eocene Thermal Maximum at Sand Creek Divide, Southern Bighorn Basin, Wyoming* (Vol. 36, pp. 1–122). University of Michigan Papers on Paleontology.

Schankler, D. M. (1980). Faunal zonation of the Willwood Formation in the central Bighorn Basin, Wyoming. In P. D. Gingerich (Ed.), *Early Cenozoic paleontology and stratigraphy of the Bighorn Basin, Wyoming* (Vol. 24, pp. 99–114). University of Michigan Papers on Paleontology.

Schankler, D. M. (1981). Local extinction and ecological re-entry of early Eocene mammals. *Nature*, *293*(5828), 135. https://doi.org/10.1038/293135a0

Scheihing, M. H., & Pfefferkorn, H. W. (1984). The taphonomy of land plants in the Orinoco Delta: A model for the incorporation of plant parts in clastic sediments of Late Carboniferous age of Euramerica. *Review of Palaeobotany and Palynology*, *41*(3–4), 205–240. https://doi.org/10.1016/0034-6667(84)90047-2

Schumer, R., & Jerolmack, D. J. (2009). Real and apparent changes in sediment deposition rates through time. *Journal of Geophysical Research*, *114*(F3). https://doi.org/10.1029/2009JF001266

Secord, R., Bloch, J. I., Chester, S. G., Boyer, D. M., Wood, A. R., Wing, S. L., et al. (2012). Evolution of the earliest horses driven by climate change in the Paleocene-Eocene Thermal Maximum. *Science*, *335*(6071), 959–962. https://doi.org/10.1126/science.1213859

Secord, R., Gingerich, P. D., Lohmann, K. C., & MacLeod, K. G. (2010). Continental warming preceding the Palaeocene–Eocene thermal maximum. *Nature*, *467*(7318), 955–958. https://doi.org/10.1038/nature09441

Shields, C. A., Kiehl, J. T., Rush, W., Rothstein, M., & Snyder, M. A. (2021). Atmospheric rivers in high-resolution simulations of the Paleocene Eocene Thermal Maximum (PETM). *Palaeogeography, Palaeoclimatology, Palaeoecology*, *567*, 110293. https://doi.org/10.1016/j.palaeo.2021.110293

Sluijs, A., Bowen, G. J., Brinkhuis, H., Lourens, L. J., & Thomas, E. (2007). The Palaeocene-Eocene Thermal Maximum super greenhouse: Biotic. Deep-time perspectives on climate change: Marrying the signal from computer models and biological proxies (p. 323). https://doi.org/10.1144/TMS002.15

Smith, F. A., Wing, S. L., & Freeman, K. H. (2007). Magnitude of the carbon isotope excursion at the Paleocene–Eocene thermal maximum: The role of plant community change. *Earth and Planetary Science Letters*, *262*(1–2), 50–65. https://doi.org/10.1016/j.epsl.2007.07.021

Smith, J. J., Hasiotis, S. T., Kraus, M. J., & Woody, D. T. (2008). Relationship of floodplain ichnocoenoses to paleopedology, paleohydrology, and paleoclimate in the Willwood Formation, Wyoming, during the Paleocene–Eocene Thermal Maximum. *Palaios*, *23*(10), 683–699. https://doi.org/10.2110/palo.2007.p07-080r

Snell, K. E., Thrasher, B. L., Eiler, J. M., Koch, P. L., Sloan, L. C., & Tabor, N. J. (2013). Hot summers in the Bighorn Basin during the early Paleogene. *Geology*, *41*(1), 55–58. https://doi.org/10.1130/G33567.1

Stanley, E. A. (1965). Upper Cretaceous and Paleocene plant microfossils and Paleocene dinoflagellates and hystrichosphaerids from northwestern South Dakota. *Bulletin of the American Paleontologist*, *49*(222), 179–384.

Strait, S. G. (2001). New Wa-0 mammalian fauna from Castle Gardens in the southeastern Bighorn Basin. In P. D. Gingerich (Ed.), *Paleocene-Eocene Stratigraphy and Biotic Change in the Bighorn and Clarks Fork Basins, Wyoming* (Vol. 33, pp. 127–143). University of Michigan Papers on Paleontology.

Tierney, J. E., Zhu, J., Li, M., Ridgwell, A., Hakim, G. J., Poulsen, C. J., et al. (2022). Spatial patterns of climate change across the Paleocene–Eocene Thermal Maximum. *Proceedings of the National Academy of Sciences*, *119*(42). https://doi.org/10.1073/pnas.2205326119

Tryon, A. F., & Lugardon, B. (2012). *Spores of the Pteridophyta: Surface, wall structure, and diversity based on electron microscope studies*. Springer Science & Business Media.

Tryon, R. M., & Tryon, A. F. (2012). *Ferns and allied plants: With special reference to tropical America*. Springer Science & Business Media.

van der Meulen, B., Gingerich, P. D., Lourens, L. J., Meijer, N., van Broekhuizen, S., van Ginneken, S., & Abels, H. A. (2020). Carbon isotope and mammal recovery from extreme greenhouse warming at the Paleocene–Eocene boundary in astronomically-calibrated fluvial strata, Bighorn Basin, Wyoming, USA. *Earth and Planetary Science Letters*, *534*, 116044. https://doi.org/10.1016/j.epsl.2019.116044

Welch, J. L., Foreman, B. Z., Malone, D., & Craddock, J. (2022). Provenance of early Paleogene strata in the Bighorn Basin (Wyoming, USA): Implications for Laramide tectonism and basin-scale stratigraphic patterns. *Tectonic Evolution of the Sevier-Laramide Hinterland, Thrust Belt, and Foreland, and Postorogenic Slab Rollback (180–20 Ma)*. https://doi.org/10.1130/2022.2555(09)

Westerhold, T., Röhl, U., Donner, B., & Zachos, J. C. (2018). Global extent of early Eocene hyperthermal events: A new Pacific benthic foraminiferal isotope record from Shatsky Rise (ODP Site 1209). *Paleoceanography and Paleoclimatology*, *33*(6), 626–642. https://doi.org/10.1029/2017PA003306

Westerhold, T., Röhl, U., Frederichs, T., Agnini, C., Raffi, I., Zachos, J. C., & Wilkens, R. H. (2017). Astronomical calibration of the Ypresian timescale: Implications for seafloor spreading rates and the chaotic behavior of the solar system? *Climate of the Past*, *13*(9), 1129–1152. https://doi.org/10.5194/cp-13-1129-2017

Wilf, P. (2000). Late Paleocene–early Eocene climate changes in southwestern Wyoming: Paleobotanical analysis. *Geological Society of America Bulletin*, *112*(2), 292–307. https://doi.org/10.1130/0016-7606(2000)112<292:lpecci>2.0.co;2

Wing, S. L. (1980). Fossil floras and plant-bearing beds of the central Bighorn Basin. In *Early Cenozoic paleontology and stratigraphy of the Bighorn Basin, Wyoming*. *Museum of Paleontology* (Vol. 24, pp. 119–125). The University of Michigan Papers on Paleontology.

Wing, S. L. (1984). Relation of paleovegetation to geometry and cyclicity of some fluvial carbonaceous deposits. *Journal of Sedimentary Research*, *54*(1), 52–66. https://doi.org/10.1306/212f83a0-2b24-11d7-8648000102c1865d

Wing, S. L. (1998). *Late Paleocene–early Eocene floral and climatic change in the Bighorn Basin, Wyoming*. *Late Paleocene–Early Eocene Biotic and Climatic Events* (Vol. 380, p. 400). Columbia University Press.

Wing, S. L., Bloch, J. I., Bowen, G. J., Boyer, D. M., Chester, S., Diefendorf, A. F., et al. (2009). Coordinated sedimentary and biotic change during the Paleocene-Eocene Thermal Maximum in the Bighorn Basin, Wyoming, USA. In *Climatic and Biotic Events of the Paleogene (CBEP 2009), extended abstracts from an international conference in Wellington, New Zealand, 12–15 January 2009*. Institute of Geological and Nuclear Sciences Limited.

Wing, S. L., & Currano, E. D. (2013). Plant response to a global greenhouse event 56 million years ago. *American Journal of Botany*, *100*(7), 1234–1254. https://doi.org/10.3732/ajb.1200554

Wing, S. L., & Greenwood, D. R. (1993). Fossils and fossil climate: The case for equable continental interiors in the Eocene. *Philosophical Transactions of the Royal Society of London. Series B: Biological Sciences*, *341*(1297), 243–252.

Wing, S. L., & Harrington, G. J. (2001). Floral response to rapid warming in the earliest Eocene and implications for concurrent faunal change. *Paleobiology*, *27*(3), 539–563. https://doi.org/10.1666/0094-8373(2001)027<0539:frtrwi>2.0.co;2

Wing, S. L., Harrington, G. J., Bowen, G. J., & Koch, P. L. (2003). Floral change during the Initial Eocene Thermal Maximum in the Powder River Basin, Wyoming. In S. L. Wing, P. D. Gingerich, B. Schmitz, & E. Thomas (Eds.), *Causes and Consequences of early Paleogene Warm Climates* (Vol. 369, pp. 425–440). Geological Society of America Special Paper.

Wing, S. L., Harrington, G. J., Smith, F. A., Bloch, J. I., Boyer, D. M., & Freeman, K. H. (2005). Transient floral change and rapid global warming at the Paleocene-Eocene boundary. *Science*, *310*(5750), 993–996. https://doi.org/10.1126/science.1116913

Wing, S. L., & Hickey, L. J. (1984). The *Platycarya* perplex and the evolution of the Juglandaceae. *American Journal of Botany*, *71*(3), 388–411. https://doi.org/10.1002/j.1537-2197.1984.tb12525.x

Wing, S. L., Morse, P. E., Vitek, N., Bloch, J. I., Korasidis, V., Baczynski, A. A., et al. (2021). An earliest Eocene conglomerate in the Bighorn Basin, Wyoming, and possible relationship to the Paleocene-Eocene Thermal Maximum. *Geological Society of America Abstracts*, *53*, 6.

Wolfe, J. A. (1995). Paleoclimatic estimates from Tertiary leaf assemblages. *Annual Review of Earth and Planetary Sciences*, *23*(1), 119–142. https://doi.org/10.1146/annurev.ea.23.050195.001003

Woody, D. T., Smith, J. J., Kraus, M. J., & Hasiotis, S. T. (2014). Manganese-bearing rhizocretions in the Willwood Formation, Wyoming, USA: Implications for paleoclimate during the Paleocene–Eocene Thermal Maximum. *Palaios*, *29*(6), 266–276. https://doi.org/10.2110/palo.2013.105

Yang, Z., Ma, W., Yang, X., Wang, L., Zhao, T., Liang, L., et al. (2022). Plastome phylogenomics provide new perspective into the phylogeny and evolution of Betulaceae (Fagales). *BMC Plant Biology*, *22*(1), 1–17. https://doi.org/10.1186/s12870-022-03991-1

Zachos, J. C., Lohmann, K. C., Walker, J. C., & Wise, S. W. (1993). Abrupt climate change and transient climates during the Paleogene: A marine perspective. *The Journal of Geology*, *101*(2), 191–213. https://doi.org/10.1086/648216

Zachos, J. C., Wara, M. W., Bohaty, S., Delaney, M. L., Petrizzo, M. R., Brill, A., et al. (2003). A transient rise in tropical sea surface temperature during the Paleocene-Eocene Thermal Maximum. *Science*, *302*(5650), 1551–1554. https://doi.org/10.1126/science.1090110

Zavada, M. S., & Dilcher, D. L. (1986). Comparative pollen morphology and its relationship to phylogeny of pollen in the Hamamelidae. *Annals of the Missouri Botanical Garden*, *73*(2), 348–381. https://doi.org/10.2307/2399117

Zetter, R., Farabee, M. J., Pigg, K. B., Manchester, S. R., DeVore, M. L., & Nowak, M. D. (2011). Palynoflora of the late Paleocene silicified shale at Almont, North Dakota, USA. *Palynology*, *35*(2), 179–211. https://doi.org/10.1080/01916122.2010.501164

Zhang, Q., Ree, R. H., Salamin, N., Xing, Y., & Silvestro, D. (2022). Fossil-informed models reveal a boreotropical origin and divergent evolutionary trajectories in the walnut family (Juglandaceae). *Systematic Biology*, *71*(1), 242–258. https://doi.org/10.1093/sysbio/syab030

Zhang, Q. Y., Deng, M., Bouchenak-Khelladi, Y., Zhou, Z. K., Hu, G. W., & Xing, Y. W. (2022). The diversification of the northern temperate woody flora–A case study of the Elm family (Ulmaceae) based on phylogenomic and paleobotanical evidence. *Journal of Systematics and Evolution*, *60*(4), 728–746. https://doi.org/10.1111/jse.12720

Zhu, J., Poulsen, C. J., & Tierney, J. E. (2019). Simulation of Eocene extreme warmth and high climate sensitivity through cloud feedbacks. *Science Advances*, *5*(9). https://doi.org/10.1126/sciadv.aax1874

Zizka, A., Carvalho-Sobrinho, J. G., Pennington, R. T., Queiroz, L. P., Alcantara, S., Baum, D. A., et al. (2020). Transitions between biomes are common and directional in Bombacoideae (Malvaceae). *Journal of Biogeography*, *47*(6), 1310–1321. https://doi.org/10.1111/jbi.13815

References From the Supporting Information

Diefendorf, A. F., Freeman, K. H., Wing, S. L., Currano, E. D., & Mueller, K. E. (2015). Paleogene plants fractionated carbon isotopes similar to modern plants. *Earth and Planetary Science Letters*, *429*, 33–44. https://doi.org/10.1016/j.epsl.2015.07.029

Frederiksen, N. O. (1980). *Sporomorphs from the Jackson Group (Upper Eocene) and adjacent strata of Mississippi and western Alabama* (Vol. 1084) US Government Printing Office.

Frederiksen, N. O., Ager, T. A., & Edwards, L. E. (1988). Palynology of Maastrichtian and Paleocene rocks, lower Colville River region, North Slope of Alaska. *Canadian Journal of Earth Sciences*, *25*(4), 512–527. https://doi.org/10.1139/e88-051

Frederiksen, N. O., & Christopher, R. A. (1978). Taxonomy and biostratigraphy of Late Cretaceous and Paleogene triatriate pollen from South Carolina. *Palynology*, *2*(1), 113–145. https://doi.org/10.1080/01916122.1978.9989168

Harrington, G. J., & Kemp, S. J. (2001). US Gulf Coast vegetation dynamics during the latest Paleocene. *Palaeogeography, Palaeoclimatology, Palaeoecology*, *167*(1–2), 1–21. https://doi.org/10.1016/s0031-0182(00)00228-5

Jaramillo, C. A., Moreno, E., Ramírez, V., da Silva-Caminha, S. A., de la Barrera, A., de la Barrera, A., et al. (2014). *Palynological record of the last 20 million years in Panama*. *Paleobotany and biogeography: A festschrift for Alan Graham in his 80th year* (pp. 124–253). Missouri Botanical Garden Press.

Secord, R., Gingerich, P. D., Smith, M. E., Clyde, W. C., Wilf, P., & Singer, B. S. (2006). Geochronology and mammalian biostratigraphy of middle and upper Paleocene continental strata, Bighorn Basin, Wyoming. *American Journal of Science*, *306*(4), 211–245. https://doi.org/10.2475/ajs.306.4.211

Smith, V., Warny, S., Jarzen, D. M., Demchuk, T., & Vajda, V. (2020). Palaeocene–Eocene miospores from the Chicxulub impact crater, Mexico. Part 1: Spores and gymnosperm pollen. *Palynology*, *44*(3), 473–487. https://doi.org/10.1080/01916122.2019.1630860

Stockey, R. A., & Manchester, S. R. (1988). A fossil flower with *in situ Pistillipollenites* from the Eocene of British Columbia. *Canadian Journal of Botany*, *66*(2), 313–318. https://doi.org/10.1139/b88-051

Wodehouse, R. P. (1933). Tertiary pollen-II The oil shales of the Eocene Green River formation. *Bulletin of the Torrey Botanical Club*, *60*(7), 479–524. https://doi.org/10.2307/2480586

Worobiec, E., Widera, M., Worobiec, G., & Kurdziel, B. (2021). Middle Miocene palynoflora from the Adamów lignite deposit, central Poland. *Palynology*, *45*(1), 59–71. https://doi.org/10.1080/01916122.2019.1697388